



NAVAL POSTGRADUATE SCHOOL

MONTEREY, CALIFORNIA

THESIS

**DIGITAL PHASED ARRAY ARCHITECTURES FOR
RADAR AND COMMUNICATIONS BASED ON OFF-THE-
SHELF WIRELESS TECHNOLOGIES**

by

Ong, Chin Siang

December 2004

Co-Advisor:

Co-Advisor:

Second Reader:

David C. Jenn

Siew Yam Yeo

Jeffrey Knorr

Approved for public release; distribution is unlimited.

THIS PAGE INTENTIONALLY LEFT BLANK

REPORT DOCUMENTATION PAGE			<i>Form Approved OMB No. 0704-0188</i>	
Public reporting burden for this collection of information is estimated to average 1 hour per response, including the time for reviewing instruction, searching existing data sources, gathering and maintaining the data needed, and completing and reviewing the collection of information. Send comments regarding this burden estimate or any other aspect of this collection of information, including suggestions for reducing this burden, to Washington headquarters Services, Directorate for Information Operations and Reports, 1215 Jefferson Davis Highway, Suite 1204, Arlington, VA 22202-4302, and to the Office of Management and Budget, Paperwork Reduction Project (0704-0188) Washington DC 20503.				
1. AGENCY USE ONLY (Leave blank)		2. REPORT DATE December 2004	3. REPORT TYPE AND DATES COVERED Master's Thesis	
4. TITLE AND SUBTITLE: Digital Phased Array Architectures for Radar and Communications Based on Off-the-Shelf Wireless Technologies			5. FUNDING NUMBERS	
6. AUTHOR(S) Ong, Chin Siang				
7. PERFORMING ORGANIZATION NAME(S) AND ADDRESS(ES) Naval Postgraduate School Monterey, CA 93943-5000			8. PERFORMING ORGANIZATION REPORT NUMBER	
9. SPONSORING /MONITORING AGENCY NAME(S) AND ADDRESS(ES) N/A			10. SPONSORING/MONITORING AGENCY REPORT NUMBER	
11. SUPPLEMENTARY NOTES The views expressed in this thesis are those of the author and do not reflect the official policy or position of the Department of Defense or the U.S. Government.				
12a. DISTRIBUTION / AVAILABILITY STATEMENT Approved for public release; distribution is unlimited.			12b. DISTRIBUTION CODE	
13. ABSTRACT (maximum 200 words) This thesis is a continuation of the design and development of a three-dimensional 2.4 GHz digital phased array radar antenna. A commercial off-the-shelf quadrature modulator and demodulator were used as phase shifters in the digital transmit and receive arrays. The phase response characteristic of the demodulator was measured and the results show that the phase difference between the received phase and transmit phase is small. In order to increase the bandwidth of the phased array, a method of time-varying phase weights for linear frequency modulated signal was investigated. Using time-varying phase weights on transmit and receive give the best performance, but require the range information of the target. It is more practical to use time-varying phase weights on only one side (transmit or receive but not both), and constant phase weights on the other side. The simulation results showed that by using time-varying phase weights, the matched filter loss is not as severe as it is when using the conventional fixed weights technique. It was also found that this method is only effective for small scan angles when the time-bandwidth product is large. The approach to implement time-varying phase weights on transmit using commercial components such as direct digital synthesizer and quadrature modulator is discussed.				
14. SUBJECT TERMS Phased Array, Radar, Antenna, Transmitter, Digital Receiver, Quadrature Demodulation, COTS.			15. NUMBER OF PAGES 83	
			16. PRICE CODE	
17. SECURITY CLASSIFICATION OF REPORT Unclassified	18. SECURITY CLASSIFICATION OF THIS PAGE Unclassified	19. SECURITY CLASSIFICATION OF ABSTRACT Unclassified	20. LIMITATION OF ABSTRACT UL	

THIS PAGE INTENTIONALLY LEFT BLANK

Approved for public release; distribution is unlimited.

**DIGITAL PHASED ARRAY ARCHITECTURES FOR RADAR AND
COMMUNICATIONS BASED ON OFF-THE-SHELF WIRELESS
TECHNOLOGIES**

Chin Siang Ong

Civilian, Ministry of Defense, Singapore

B.E.(Electrical Engineering), National University of Singapore, 1998

Master of Engineering (Electrical Engineering), National University of Singapore, 2002

Submitted in partial fulfillment of the
requirements for the degree of

MASTER OF SCIENCE IN ELECTRICAL ENGINEERING

from the

**NAVAL POSTGRADUATE SCHOOL
December 2004**

Author: Chin Siang Ong

Approved by: David C. Jenn
Co-Advisor

Siew Yam Yeo
Co-Advisor

Jeffrey Knorr
Second Reader

John P. Powers
Chairman, Department of Electrical and Computer Engineering

THIS PAGE INTENTIONALLY LEFT BLANK

ABSTRACT

This thesis is a continuation of the design and development of a three-dimensional 2.4 GHz digital phased array radar antenna. A commercial off-the-shelf quadrature modulator and demodulator were used as phase shifters in the digital transmit and receive arrays. The phase response characteristic of the demodulator was measured and the results show that the phase difference between the received phase and transmit phase is small. In order to increase the bandwidth of the phased array, a method of time-varying phase weights for linear frequency modulated signal was investigated. Using time-varying phase weights on transmit and receive give the best performance, but require the range information of the target. It is more practical to use time-varying phase weights on only one side (transmit or receive but not both), and constant phase weights on the other side. The simulation results showed that by using time-varying phase weights, the matched filter loss is not as severe as it is when using the conventional fixed weights technique. It was also found that this method is only effective for small scan angles when the time-bandwidth product is large. The approach to implement time-varying phase weights on transmit using commercial components such as direct digital synthesizer and quadrature modulator is discussed.

THIS PAGE INTENTIONALLY LEFT BLANK

TABLE OF CONTENTS

I.	INTRODUCTION.....	1
A.	BACKGROUND	1
B.	SCOPE OF THE THESIS.....	2
C.	ORGANIZATION OF THE THESIS	3
II.	BASIC LINEAR PHASED ARRAY CHARACTERISTICS	5
A.	ARRAY FACTOR FOR A LINEAR PHASED ARRAY	5
B.	GRATING LOBES AND MUTUAL COUPLING	7
1.	Grating Lobes.....	7
2.	Mutual Coupling	8
C.	ARRAY BANDWIDTH	8
D.	QUADRATURE DEMODULATION.....	12
E.	DIGITAL PHASED ARRAY TRANSMITTER AND RECEIVER ARCHITECTURE.....	13
F.	SUMMARY	15
III.	MEASUREMENT AND SIMULATION RESULTS ANALYSIS	17
A.	PHASE CHARACTERISTICS OF QUADRATURE DEMODULATOR	17
1.	AD8347EVAL Quadrature Demodulator Board.....	18
2.	Experimental Setup	19
3.	Experimental Results.....	21
B.	SIMULATION RESULTS USING TIME-VARYING PHASE WEIGHTS	25
1.	Preliminary Investigation of Using Time-varying Phase Weights on Transmit	26
2.	Comparison of Phase Weighting Methods for LFM Signals	28
3.	Loss in Signal-to-Noise Ratio (SNR) Comparison for Different Types of Phase Weights.....	32
C.	APPROACH TO IMPLEMENT TIME-VARYING PHASE WEIGHTS ON TRANSMIT USING COTS COMPONENTS	33
1.	Laboratory Setup for Transmit Architecture	33
a.	AD9854EVAL Direct Digital Synthesizer	35
b.	Fabrication of Step-up Transformer.....	39
2.	Preliminary Results	40
a.	Simulation Result of I and Q Phase and Amplitude Imbalance	43
3.	Future Work.....	44
D.	SUMMARY	45
IV.	CONCLUSIONS AND FUTURE WORK	47
A.	CONCLUSIONS	47
B.	SUGGESTIONS FOR FUTURE WORK.....	48

1.	Implement Time-varying Phase Weights on the Transmit Side....	48
2.	Arrays Transmit and Receive Antenna with Time Delay Units....	48
3.	Time Delay Beam-steering	48
APPENDIX A: MATLAB CODES		49
APPENDIX B: PHASE RESPONSE OF DEMODULATOR WITH AGC MODE TURNED ON.....		59
LIST OF REFERENCES		63
INITIAL DISTRIBUTION LIST		65

LIST OF FIGURES

Figure 1.	Artist's concept of the integrated superstructure for the DD(X) (From Ref. [2].).....	1
Figure 2.	An equally spaced linear array with N elements.....	5
Figure 3.	Beam pattern of a 16-element linear phased array with scan angle at 30 degrees.	7
Figure 4.	Beam patterns for a phased array at 0.8 GHz, 1.7 GHz and 2.5 GHz when phase shifters are set to steer beam to 20 degrees at 1.7 GHz.	9
Figure 5.	In-phase and quadrature demodulation block diagram (After Ref. [13].).....	13
Figure 6.	Architecture of a digital phased array transmitter (From Ref. [4].).....	14
Figure 7.	Architecture of a digital phased array receiver (From Ref. [4].).....	15
Figure 8.	AD8347EVAL block diagram (From Ref. [13].).....	18
Figure 9.	Experimental setup to measure the phase response of AD8347EVAL demodulator board (From Ref. [4].).....	19
Figure 10.	Signal connections to AD8347EVAL board (After Ref. [4].).....	20
Figure 11.	Measured differential I and Q components versus transmitted phase with VGIN set to 0.7 V and AGC mode turned off.	23
Figure 12.	Received phase versus transmitted phase with VGIN set to 0.7 V and AGC mode turned off.	24
Figure 13.	Phase error versus transmitted phase with VGIN set at 0.7 V and AGC mode turned off.....	25
Figure 14.	Radiation patterns of a linear array using constant and time-varying phase weights.	27
Figure 15.	Matched filter output of LFM signal for 16-element linear array, $BT = 850$, with constant phase weights on transmit and receive, at different scan angles.	28
Figure 16.	Matched filter output of LFM signal for 16-element linear array, $BT = 850$, with time-varying phase weights for transmit and constant phase weights for receive, at different scan angles.....	29
Figure 17.	Matched filter output of LFM signal for 16-element linear array, $BT = 850$, with time-varying phase weights for both transmit and receive, at different scan angles.	29
Figure 18.	Matched filter output of LFM signal for 16-element linear array, $BT = 1360$, with constant phase weights both transmit and receive, at different scan angles.	31
Figure 19.	Matched filter output of LFM signal for sixteen-element linear array, $BT = 1360$, with time-varying phase weights on transmit and constant phase weights on receive at different scan angles.	32
Figure 20.	Comparison of loss in SNR between using time-varying phase weights and constant phase weights for receive, and constant phase weights for both transmit and receive.	33

Figure 21.	Quadrature DDS SSB upconversion using AD9854 and AD8346 (From Ref. [14].).....	34
Figure 22.	Laboratory setup for SSB upconversion (After Ref. [14].).....	35
Figure 23.	Block diagram of AD9854 DDS (From Ref. [15].).....	36
Figure 24.	AD9854EVAL evaluation software (version 1.72) GUI.	37
Figure 25.	AD9854EVAL cable and signal connections.	38
Figure 26.	Schematic diagram of center-tapped impedance step-up transformer (After Ref. [14].).....	39
Figure 27.	Board diagram for the step up transformer.	40
Figure 28.	Frequency spectrum output of AD8346EVAL at center frequency equal to 1.9 GHz.	41
Figure 29.	Frequency spectrum output of AD8346EVAL at center frequency equal to 2.1 GHz.	42
Figure 30.	Effect of I and Q amplitude and phase imbalance.	44
Figure 31.	Proposed experimental setup for time-varying phase weights on transmit and constant phase weights on receive.	45
Figure 32.	Measured Differential I and Q components versus transmitted phase with AGC mode turned on.	61
Figure 33.	Demodulated phase versus transmitted phase with AGC mode turned on.	62
Figure 34.	Phase error versus transmitted phase with AGC mode turned on.	62

LIST OF TABLES

Table 1.	Measurement results of AD8347EVAL Quadrature demodulator board.	22
Table 2.	Parameters used in simulation.	26
Table 3.	Parameters used in the matched filter calculation for LFM signals.....	30
Table 4.	Parameters used in the design of microstrip transmission line.	40
Table 5.	Parameters used for Figure 28.	41
Table 6.	Parameters used for Figure 29.	42
Table 7.	Measurement results of AD8347EVAL Quadrature demodulator board with AGC mode turned on.	60

THIS PAGE INTENTIONALLY LEFT BLANK

ACKNOWLEDGMENTS

I would like to express my deepest appreciation and gratitude to Professor David Jenn for his patience, guidance and advice throughout the entire duration of this thesis. I would like to thank Mr. Siew Yam, Yeo for taking time off from his busy schedule to guide me and share his knowledge in this research area. I would also like to thank Professor Jeffrey Knorr for his instructions and comments on this thesis. Last but not the least, to my wonderful wife, Jia Miin, and my baby boy, Chi Juay, for their love, patience and understanding.

THIS PAGE INTENTIONALLY LEFT BLANK

EXECUTIVE SUMMARY

Phased array systems play an important part in defining the type of radar and communications systems that will be installed on the next generation military platforms. Examples of next generation military platforms that use phased array systems are the new surface combatant ships, Joint Strike Fighter and Milstar satellite communication systems.

Phased array systems are typically complex and required a large number of specially designed and integrated components. It is therefore beneficial to leverage on low-cost and high-performance commercial components for building such a system.

Some of the advantages of phased array systems are given below:

1. Agile and fast beam steering can be achieved since the beam is steered electronically, which allows the switching to be completed in a very short time.
2. It has the ability to track multiple targets. This is because the phased array is able to generate multiple independent beams at the same time to track different targets.
3. It does not contain any mechanical parts, which increases the overall antenna mean time before failure.
4. It can be designed to conform to the shape of the platform and hence does not affect the aerodynamic or ocean dynamic performance of the platform.
5. It allows graceful degradation of performance when some of the antenna elements malfunction.
6. It can be used for wideband applications. This can be achieved by adjusting the values of the phase shifters at different frequencies.

This thesis is a continuation of the design and development of a three-dimensional 2.4-GHz digital phased array radar antenna. This thesis investigated the periodic phase error that was attributed to a commercial modulator used in the previous research. Further

investigation indicated that this error arose due to the inappropriate operating conditions of the commercial demodulator board. After the correct operating conditions were used, the periodic phase errors disappeared, and the results from the phase response of the demodulator showed that the phase difference between the received and transmitted phases, which ideally should be zero, was acceptably small.

In order to improve the phase distortion and increase the operating bandwidth of the phased array, this thesis investigated a technique of using different types of time-varying phase weights for a linear frequency modulated signal on both transmit and receive. Using time-varying phase weights on both transmit and receive gives the best performance, but requires range information. It is therefore more practical to use time-varying phase weights on one side (either the transmit or receive, but not both), and constant phase weights on the other side. The results also show that this technique is only effective for small scan angles when the time-bandwidth product is high. Results show that using time-varying phase weights improves the signal-to-noise ratio performance.

The approach to implement the time-varying phase weights on the transmit side using commercial components is presented. The components used include a direct digital synthesizer and a quadrature modulator. The laboratory results showed that a bandpass filter is required to suppress the image signal.

I. INTRODUCTION

A. BACKGROUND

Phased arrays have been used widely in both civilian and military applications. In civilian applications, they can be found in areas such as air traffic control, smart antennas and satellite communications. As for the military applications, phased arrays have been used in areas such as radar, communications, electronic warfare (EW) and missile guidance. Currently, phased array systems play an important role in defining the type of radar and communications system that will be installed on the next generation military platforms. Examples of next generation military platforms that use phased array systems are the new surface combatant ships DD(X), the Joint Strike Fighter (JSF) and the Milstar satellite communications system.

On the DD(X) program, a new Multi-Function Radar (MFR), the AN/SPY-3 [1], a X-band active phased array radar, is designed to support the horizon search and fire control requirements for the next generation destroyers. In addition, the low signature electronically steered phased array is designed to be embedded into the composite superstructure as shown in Figure 1. The array elements for other onboard communication systems are also embedded within the superstructure. This kind of “all in one” superstructure design allows the DD(X) to achieve a significant reduction in Radar Cross Section (RCS).

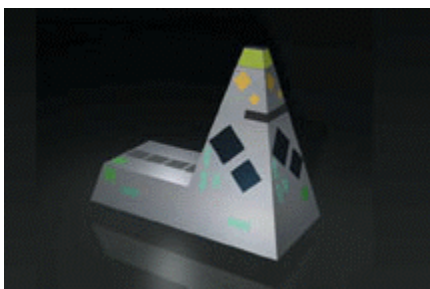


Figure 1. Artist's concept of the integrated superstructure for the DD(X) (From Ref. [2].).

Phased array antennas have many advantages over antennas that make use of mechanical scanning to steer the main beam [2]. Some of the advantages are the following:

1. Agile and fast beam steering can be achieved since the beam is steered electronically, which allows the switching to be completed in a very short time.
2. It has the ability to track multiple targets. This is because the phased array is able to generate multiple independent beams at the same time to track different targets.
3. It does not contain any mechanical parts, which increases the overall antenna Mean Time Before Failure (MTBF).
4. It can be designed to conform to the shape of the platform and hence does not affect the aerodynamic or ocean dynamic performance of the platform.
5. It allows graceful degradation of performance when some of the antenna elements malfunction.
6. It can be used for wideband applications. This can be achieved by adjusting the values of the phase shifters at different frequencies.

The design of a phased array radar system is complex since it involves controlling hundreds or sometimes thousands of antenna elements. Phased arrays generally cost more than conventional arrays because they require a large number of specially designed and integrated components, such as phase shifters and antenna elements.

With the rapid technology advancement and cost reduction that can be offered by Commercial-off-the-Shelf (COTS) electronic components, defense system designers are now looking at areas to use COTS components, so as to keep costs to a minimum without compromising on the performance. Phased array radar systems are one of the many candidates that can leverage on the COTS products to reduce cost and still achieve a relatively good performance.

B. SCOPE OF THE THESIS

This thesis is a continuation of the design and development of a three-dimensional 2.4-GHz digital phased array antenna started in [3] and continued in [4]. The main objective of this research was to address some of the design issues that were identified based

on the results found in [4]. These issues include a periodic phase error caused by the commercial modulator and achieving wideband performance for the phased array using commercial modulators and demodulators.

In [4], the bandwidth characteristics of the Analog Devices AD8346EVAL Quadrature Modulator board were investigated. It was shown that the modulator board is not able to provide wide instantaneous bandwidth. The Analog Devices AD8347EVAL Demodulator board was able to be configured to operate as a phase shifter. The phase response from the demodulator was measured and compared with the transmitted phase. At that time the phase difference between the measured phase response and the transmitted phase was attributed to the modulator board. Further investigation indicated that this was not the case, but was due to a measurement error. In the first part of this thesis, the actual cause of the phase error found in [4] is further investigated and new results are presented.

Next, an approach, proposed in [5] and [6], to reduce array dispersion and increase the operating bandwidth, was examined. The technique proposed to steer the beam for Linear Frequency Modulated (LFM) waveforms is to introduce time-varying phase weights. The simulation results using this technique are presented and discussed in this thesis. In addition, the approach to implement this technique using COTS components, such as Direct Digital Synthesizer (DDS), AD8346EVAL modulator and AD8347EVAL demodulator, is also shown.

C. ORGANIZATION OF THE THESIS

Chapter II provides an overview of the characteristics of linear phased arrays. These characteristics include calculating the Array Factor (AF), the occurrence of grating lobes, mutual coupling, and definition of the array bandwidth. Next, quadrature modulation and demodulation are also discussed. The architectures for digital phased array transmit and receive configurations are briefly described.

Chapter III provides the measured phased response of the commercial demodulator. The simulation results using the technique proposed in [5] and [6] are presented. An approach for implementing the technique using COTS components is also presented.

Chapter IV contains the summary of the results and recommendations for future research in using COTS components for digital phased arrays.

Appendix A is a list of MATLAB codes used for the simulations. Appendix B presents the results on the phase response of the demodulator with automatic gain control (AGC) mode turned on.

II. BASIC LINEAR PHASED ARRAY CHARACTERISTICS

This chapter focuses on the theory of the linear phased array and covers some of the important characteristics such as Array Factor (AF), grating lobes, mutual coupling and array bandwidth. It presents the concept of quadrature modulation and demodulation. The architectures of digital phased array transmit and receive antennas are also discussed.

A. ARRAY FACTOR FOR A LINEAR PHASED ARRAY

A linear phased array is one where the antenna elements are aligned along a straight line (the array axis). The method used to scan the main beam is by varying the phase of the individual antenna elements. Figure 2 shows a diagram of an equally spaced N -element receiving array. The spacing between two antenna elements is indicated as d in the figure. The angle θ represents the angle of arrival of the radio waves. Although the discussion in this chapter is presented in terms of the receive antenna, the formulas apply to the transmit antenna as well.

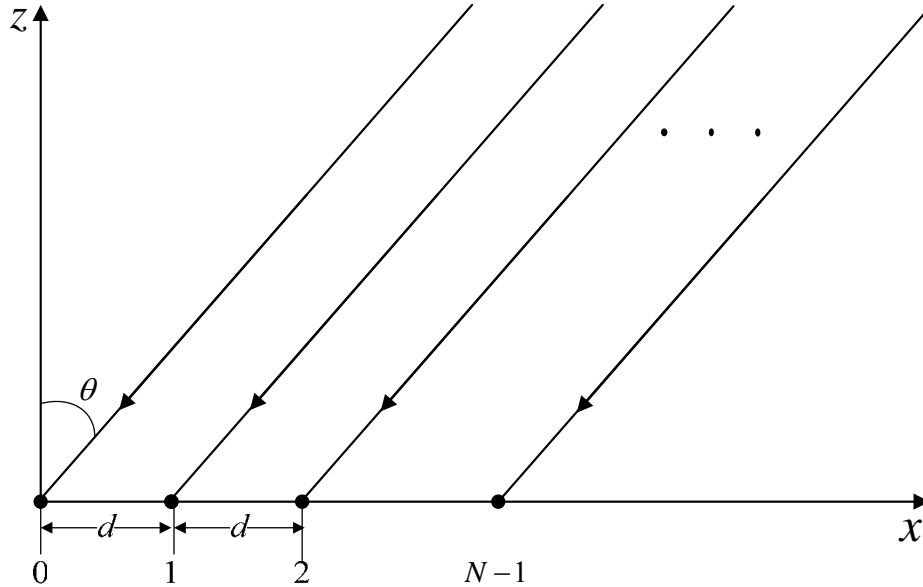


Figure 2. An equally spaced linear array with N elements.

In this thesis, the antenna elements are assumed to be uniformly excited and equally spaced. The spacing d between two antenna elements is set equal to $\lambda_o/2$, where

λ_o is the wavelength of the center frequency of the operating band f_o . Each antenna element has an amplitude and phase associated with it. Assuming each antenna element to be an isotropic point source, the array factor (AF) for an N -element array is given by [7]

$$F(\theta) = \sum_{k=0}^{N-1} A_k e^{j(\kappa k d \sin \theta + k \alpha)} \quad (1)$$

where

$\kappa = 2\pi/\lambda$ (wave number),

λ is the wavelength of the received signal,

$A_k e^{jk\alpha}$ is the complex weight of k^{th} element,

A_k is the amplitude at element k ,

α is the phase difference between k^{th} and $(k-1)^{th}$ element, and

d is the spacing between antenna elements.

For the linear antenna array to steer its main beam to angle θ_o , α must be equal to $-\kappa d \sin(\theta_o)$, so that $F(\theta)$ gives a maximum magnitude at that value. In this thesis, A_k is considered to be normalized and is set to the value 1.

Figure 3 shows the beam pattern of a sixteen-element linear phased array with uniform amplitude at 1.7 GHz for scan angle set at 30 degrees. The element spacing is set to be half the wavelength of the frequency 1.7 GHz. The main beam peak is at 30 degrees. There are $N-2$ sidelobes with the highest one about 13.2 dB below the main beam at this scan angle. It can be observed from the figure that the sidelobes are not symmetrical about the main beam when the beam is scanned.

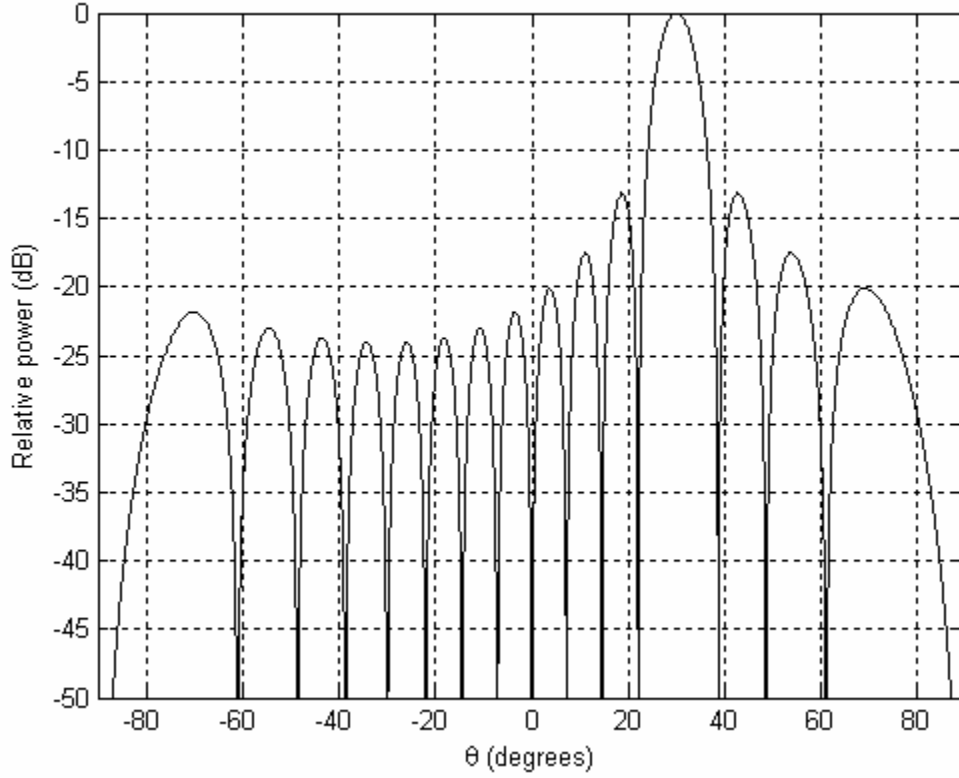


Figure 3. Beam pattern of a 16-element linear phased array with scan angle at 30 degrees.

B. GRATING LOBES AND MUTUAL COUPLING

1. Grating Lobes

The spacing between antenna elements is critical in the design of a uniformly spaced phased array. This is because when the spacing exceeds certain critical value, grating lobes will occur [8]. Grating lobes are additional sidelobes that have the same amplitude as the main beam. It is normally undesirable to have grating lobes, and in order to avoid them, the element spacing d is required to meet the condition given by

$$\frac{d}{\lambda_h} \leq \frac{1}{1 + |\sin \theta_o|} \quad (2)$$

where λ_h is the wavelength of the highest operating frequency and θ_o is the scan angle.

Based on this condition, when scanning to endfire at $\theta_o = \pm 90$ degrees, the first grating lobe will occur when the spacing is greater than $\lambda_h/2$.

2. Mutual Coupling

Mutual coupling occurs because the antenna elements within the array interact with each other. This interaction between elements results in an impedance change as seen by each element, which in turn affects the current magnitude, phase and distribution on other neighboring elements [2, 9].

In general, the element spacing d should be designed to avoid grating lobes and reduce the adverse effects of mutual coupling. According to [10] and [11], the spacing is recommended to be between 0.33λ and 0.5λ .

C. ARRAY BANDWIDTH

Normally phase shifters, rather than time delay devices, are used to steer the main beam in a phased array. This is because it can be costly to insert time delay devices for each of the antenna elements in a large array. They are also physically large, bulky and lossy.

The array factor for a narrowband signal can be represented by Equation (1). For wideband signals [12], the parameters in Equation (1) vary with frequency, so now the AF is given by

$$F(\theta, f) = \sum_{k=0}^{N-1} A_k e^{j\left(k 2\pi \frac{f}{c} d \sin \theta + 2\pi \frac{f}{c} \alpha\right)} \quad (3)$$

where f is the frequency of the signal, A_k is the amplitude at element k and c is the speed of light.

Phase shifters are designed to shift signals at a center frequency f_o and, if the signal that is being received is not at f_o , as may be the case for wideband signals, an effect called “beam squinting” will occur. An example of beam squinting is shown in Figure 4,

where the beam is first pointed to 20 degrees for $f_o = 1.7$ GHz and the frequency is then changed to 0.8 GHz and 2.5 GHz. It can be seen that the scan angle of the main beam decreases for frequencies higher than the center frequency and increases for frequencies lower than the center frequency. The beamwidth also becomes narrower at higher frequencies and wider for lower frequencies.

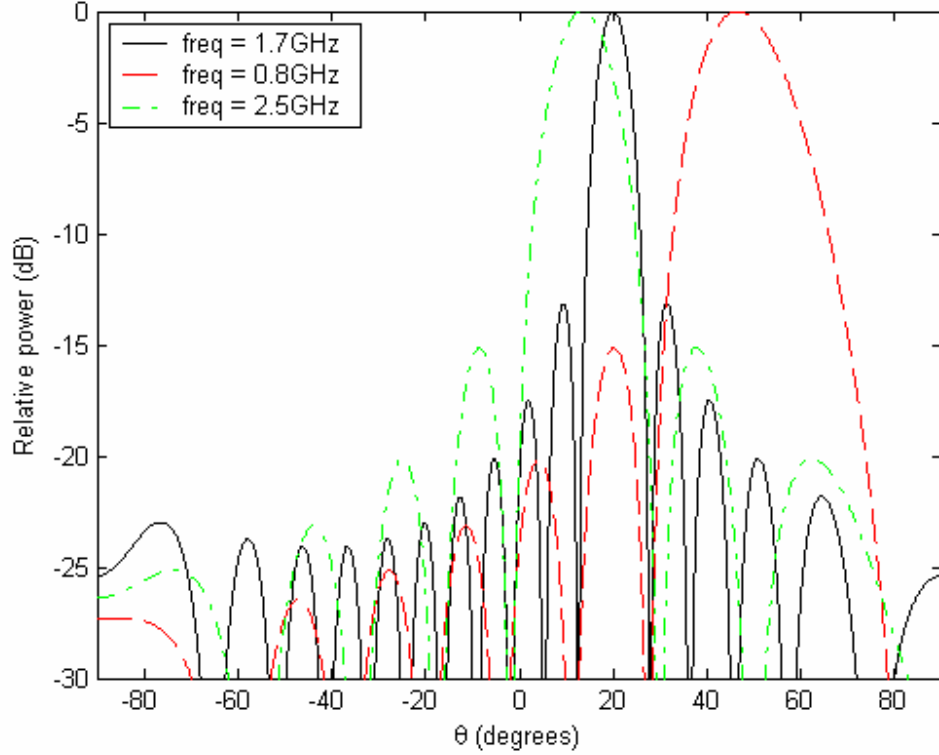


Figure 4. Beam patterns for a phased array at 0.8 GHz, 1.7 GHz and 2.5 GHz when phase shifters are set to steer beam to 20 degrees at 1.7 GHz.

Reference [2] suggests that it is possible for a phased array to achieve wideband performance by changing the settings of the phase shifters whenever the frequency of a signal with narrow instantaneous bandwidth is changed. This is equivalent to radiating multiple narrowband signals one at a time over a wide range of frequencies by adjusting the settings of the phase shifters. This suggestion is similar to the technique proposed in [5].

Reference [5] describes a technique that can improve the performance of a linear phased array that is transmitting linear frequency modulated (LFM) signals. This tech-

nique can reduce the array dispersion that is caused by the different frequency components in LFM signals and also increases the bandwidth. The equation of a LFM signal of sweep period T is given by

$$s(t) = \text{rect}\left(\frac{t}{T}\right) e^{j2\pi\left(f_o t + (\mu/2)t^2\right)} \quad (4)$$

where

$$\text{rect}\left(\frac{t}{T}\right) = \begin{cases} 1, & |t| \leq T/2 \\ 0, & |t| > T/2, \end{cases}$$

$\mu = B/T$ is the ratio of signal bandwidth to sweep period, and f_o is the center frequency.

The array factor of the linear array using time-varying weights to scan the beam to θ_o is given by

$$F(t, \theta) = \sum_{n=1}^N \alpha_n s(t - \tau_n) e^{j2\pi\phi(t, \theta)} \quad (5)$$

where

α_n is the real weight for the n -th element,

$$\tau_n = \frac{nd}{c} \sin \theta_o, \text{ and}$$

$\phi(t, \theta)$ is the phase setting.

Reference [4] has shown that the phase setting in Equation (6) is given by

$$\phi(t, \theta) = f_o \frac{nd}{c} \sin \theta_o - \frac{\mu}{2} \left(\frac{nd}{c} \sin \theta_o \right)^2 + \mu t \frac{nd}{c} \sin \theta_o. \quad (6)$$

The first two terms in Equation (7) represent the phase offsets that are required to implement the time-varying phase weights. The frequency offset that is required for the time-varying phase weights can be obtained by taking the temporal derivative of $\phi(t, \theta)$,

$$f_{\text{offset}}(n) = \frac{\mu nd}{c} \sin \theta_o. \quad (7)$$

Reference [6] describes an extension of the method introduced in [5]. Two types of phase weights on the receiving end are examined: (1) constant phase weights, and (2) time-varying phase weights. When time-varying phase weights are used for transmitting and constant phase weights are used for receiving, the array output (assuming that the scan angle is the same as target angle) is given by

$$X_{\nu\phi}(t; \theta_o, \theta_o) = e^{j2\pi(f_o t + (\mu/2)t^2)} \sum_{n=0}^{N-1} \sum_{k=0}^{N-1} \alpha_n \alpha_k \text{rect} \left\{ \frac{t - (n+k)d \sin \theta_o / c}{T} \right\} \quad (8)$$

$$\times \exp \left\{ -j2\pi \frac{\mu t k d}{c} \sin \theta_o \right\} \exp \left\{ j\pi \mu \left(\frac{k d}{c} \right)^2 \sin^2 \theta_o \right\}.$$

where the index n refers to the transmit side and k to the receive side. The first subscript on X denotes the weighting technique on transmit, whereas the second subscript denotes the weighting technique on receive. The symbol ν is for time-varying phase weights and ϕ for constant phase weights.

For the case of a conventional linear phased array, where both transmit and receive phase weights are constant, the array output is given by

$$X_{\phi\phi}(t; \theta_o, \theta_o) = e^{j2\pi(f_o t + (\mu/2)t^2)} \sum_{n=0}^{N-1} \sum_{k=0}^{N-1} \alpha_n \alpha_k \text{rect} \left\{ \frac{t - (n+k)d \sin \theta_o / c}{T} \right\} \quad (9)$$

$$\times \exp \left\{ -j2\pi \frac{(n+k)d \mu t}{c} \sin \theta_o \right\} \exp \left\{ j\pi \mu \left(\frac{(n+k)d \sin \theta_o}{c} \right)^2 \right\}.$$

If time-varying phase weights are used at the receiver, the array needs to know the exact range of the target *a priori*. This might pose a problem when the array is in the search mode. The array output for time-varying phase weights on both transmit and receive is given by

$$X_{\nu\nu}(t; \theta_o, \theta_o) = e^{j2\pi(f_o t + (\mu/2)t^2)} \sum_{n=0}^{N-1} \sum_{k=0}^{N-1} \alpha_n \alpha_k \text{rect} \left\{ \frac{t - (n+k)d \sin \theta_o / c}{T} \right\}. \quad (10)$$

By using time-varying phase weights in a linear phased array, the instantaneous bandwidth is increased as compared to using constant phase weights. The best performance occurs for the case of time-varying phase weights for both transmit and receive. However, in this case, the range of target needs to be made known to the receive array *a priori*.

D. QUADRATURE DEMODULATION

Quadrature modulation and demodulation are commonly used in radar and communications applications. After the received signal has been down converted to a base-band signal, it will be demodulated to form the in-phase (I) and quadrature (Q) components of the input signal. For a narrowband signal, the representation for the carrier signal is

$$s(t) = A(t) \cos[\omega_c t + \varphi(t)] = I(t) \cos(\omega_c t) - Q(t) \sin(\omega_c t) \quad (11)$$

where

$$\begin{aligned} I(t) &= A(t) \cos(\varphi(t)) \text{ is the in-phase component of } s(t), \\ Q(t) &= A(t) \sin(\varphi(t)) \text{ is the quadrature component of } s(t), \\ \omega_c &= 2\pi f_c, \\ f_c &\text{ is the carrier frequency,} \\ A(t) &= \text{amplitude of } s(t), \text{ and} \\ \varphi(t) &\text{ is the phase of } s(t). \end{aligned}$$

The amplitude $A(t)$ and phase $\varphi(t)$ of $s(t)$ can be calculated by using the equations given by [13] as

$$A(t) = \sqrt{I(t)^2 + Q(t)^2} \quad (12)$$

and

$$\varphi(t) = \tan^{-1} \left(\frac{Q(t)}{I(t)} \right). \quad (13)$$

Figure 5 shows an I and Q demodulation architecture where the local oscillator (LO) frequency is set to be equal to the carrier frequency, so as to produce a baseband signal. This kind of architecture is called homodyne or direct conversion detection.

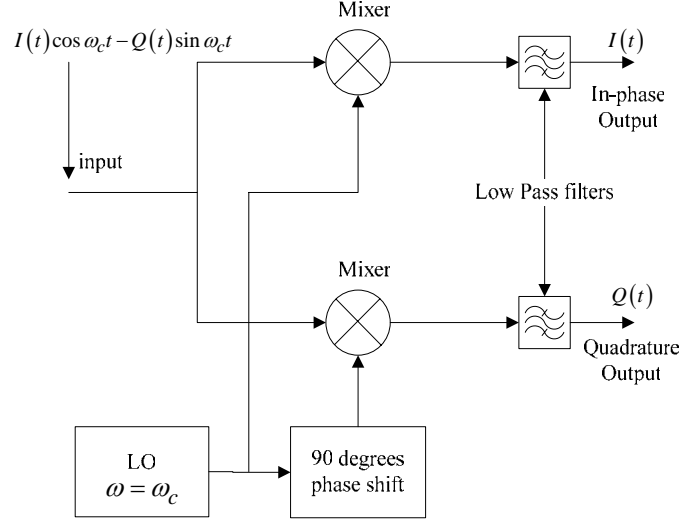


Figure 5. In-phase and quadrature demodulation block diagram (After Ref. [13]).

E. DIGITAL PHASED ARRAY TRANSMITTER AND RECEIVER ARCHITECTURE

In this section, the architectures for digital transmit and receive phased arrays are briefly described. Figure 6 shows the architecture of a digital transmit phased array. The I and Q components of the transmitted signal leave the digital-to-analog converter (DAC) and are sent to the quadrature modulator, which mixes the signal with the local oscillator (LO) carrier frequency. This signal, which is now at the carrier frequency, is then sent to the antenna element. In this research, each element has a quadrature modulator that is configured as a phase shifter.

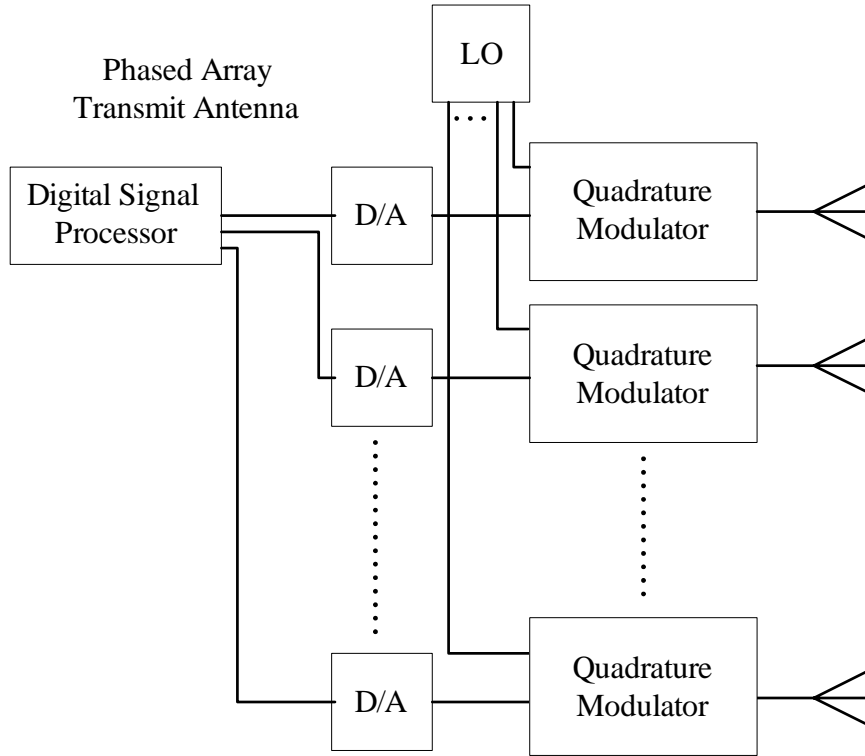


Figure 6. Architecture of a digital phased array transmitter (From Ref. [4].).

The process at the receiver end is the reverse of that used in transmitter as shown in Figure 7. The received signal is downconverted to baseband by mixing it with the LO carrier frequency in the quadrature demodulator. The outputs from the quadrature demodulator, the I and Q components of the received signal, are then sent to an analog-to-digital converter (ADC) to be digitized. The digital signal is then sent to the digital signal processor (DSP) for further processing.

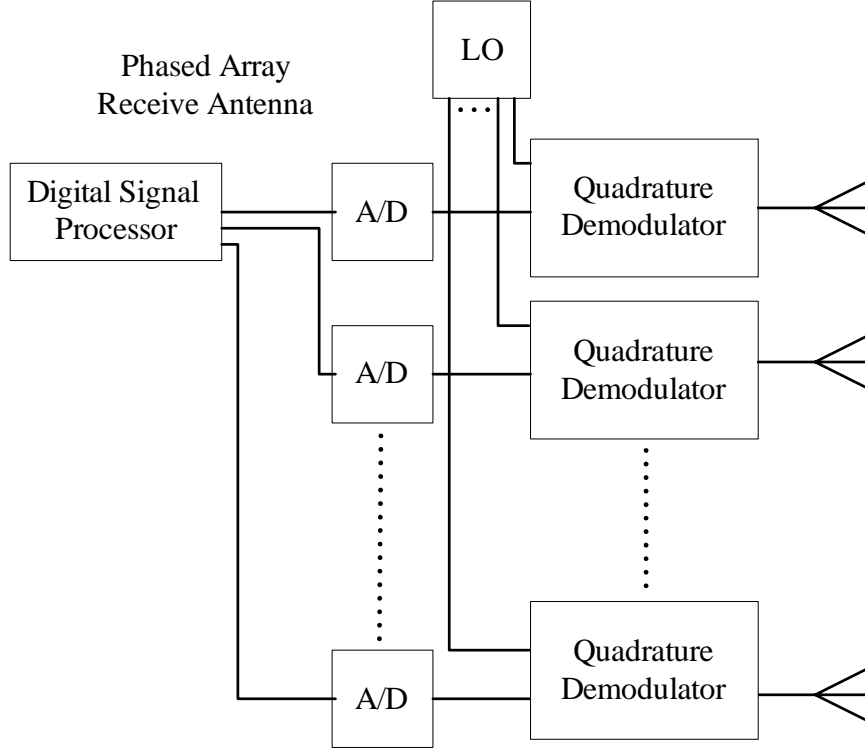


Figure 7. Architecture of a digital phased array receiver (From Ref. [4].).

F. SUMMARY

This chapter discussed the theory of a simple linear phased array. Some important characteristics of a linear array, such as array factor, grating lobes, mutual coupling, and array bandwidth were introduced. Finally, the architectures of digital transmit and receive phased arrays were also discussed.

The next chapter investigates the measurements of the phase characteristics of the commercial demodulator. Simulation results based on techniques proposed in [5] and [6] are presented and discussed.

THIS PAGE INTENTIONALLY LEFT BLANK

III. MEASUREMENT AND SIMULATION RESULTS ANALYSIS

In the first part of this chapter, the measurement results for the phase characteristic of the commercial demodulator are presented. In the second part, the simulation results based on the time-varying phase shift technique proposed in [5] and [6] are presented and discussed. A means of implementing the technique using commercial products is also proposed.

A. PHASE CHARACTERISTICS OF QUADRATURE DEMODULATOR

In the design of the three-dimensional 2.4-GHz phased array transmit antenna in [3], a commercial radio frequency (RF) modulator, the Analog Devices AD8346EVAL Quadrature modulator board, was chosen as the phase shifter. In order to receive the signals from the phased array transmit antenna, a compatible receive antenna needed to be designed using suitable COTS products. It is with this objective that in [4], the Analog Devices AD8347EVAL Quadrature demodulator board was chosen as the phase shifter at the receiver end.

From the phase response results of the demodulator presented in [4], the test setup for measuring the receive phase used a transmit modulator to introduce a phase shift to the signal sent to the demodulator. The measured received data was found to have some phase errors, which appeared to be greatest at 45° , 135° , 225° and 315° . This error was attributed to the AD8346EVAL modulator where measurements in [3] had shown that the modulator phase errors are greatest on the diagonals of the I - Q plane. However, during the course of this research, it was found that the error was due to operating the demodulator under non-optimum conditions. The detailed data on the operating characteristics of the AD8347EVAL Quadrature demodulator board can be found in [4].

In this section, the results for the phase response of AD8347EVAL Quadrature demodulator board operating under a different condition, with 0.7 V being supplied to voltage gain control input (VGIN) and AGC mode turned off, is presented and discussed.

1. AD8347EVAL Quadrature Demodulator Board

According to [13], the AD8347EVAL Quadrature demodulator board is a broadband direct quadrature demodulator with AGC amplifiers at both RF and baseband. This board contains all the components required for amplification, downconversion and filtering. The frequency range of the AD8347EVAL is from 0.8 to 2.7 GHz. It is compatible with AD8346EVAL modulator board which is being used in this research as the phase shifter on the transmit side.

The AD8347EVAL board is capable of directly downconverting a RF signal to I and Q baseband components by mixing with the LO signal. Its quadrature phase error and I/Q amplitude imbalance are ± 3 degrees and 0.3 dB from 0.8 to 2.7 GHz [13]. Figure 8 shows the block diagram of a AD8347EVAL board. The I and Q voltage outputs from this board can be measured at the in-phase output pin negative (IOPN), in-phase output pin positive (IOPP), quadrature output pin negative (QOPN) and quadrature output pin positive (QOPP) as shown in Figure 8.

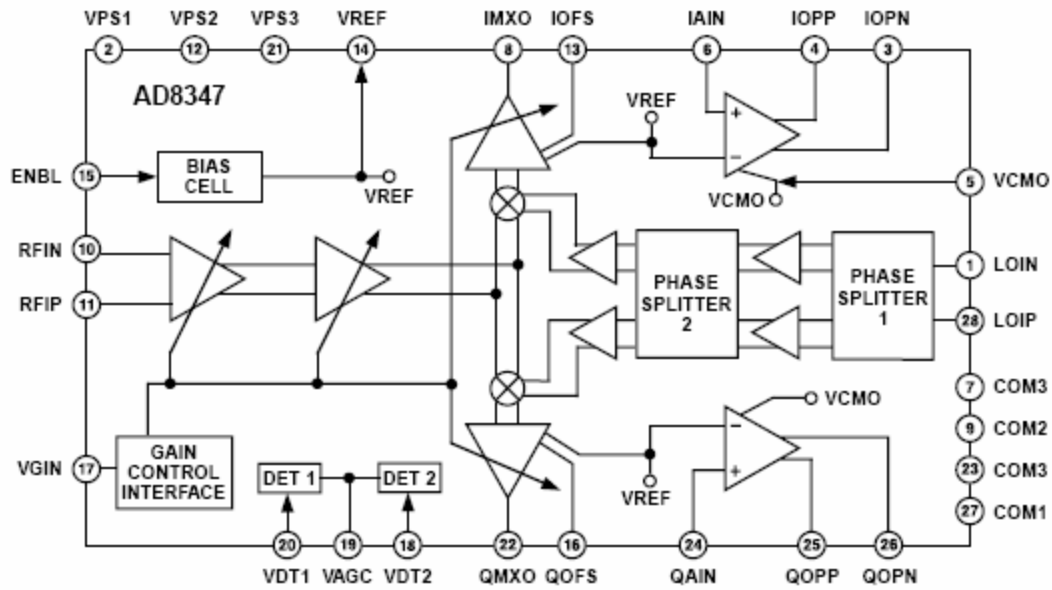


Figure 8. AD8347EVAL block diagram (From Ref. [13].).

2. Experimental Setup

The experimental setup to measure the phase response of AD8347EVAL demodulator board is shown in Figure 9.

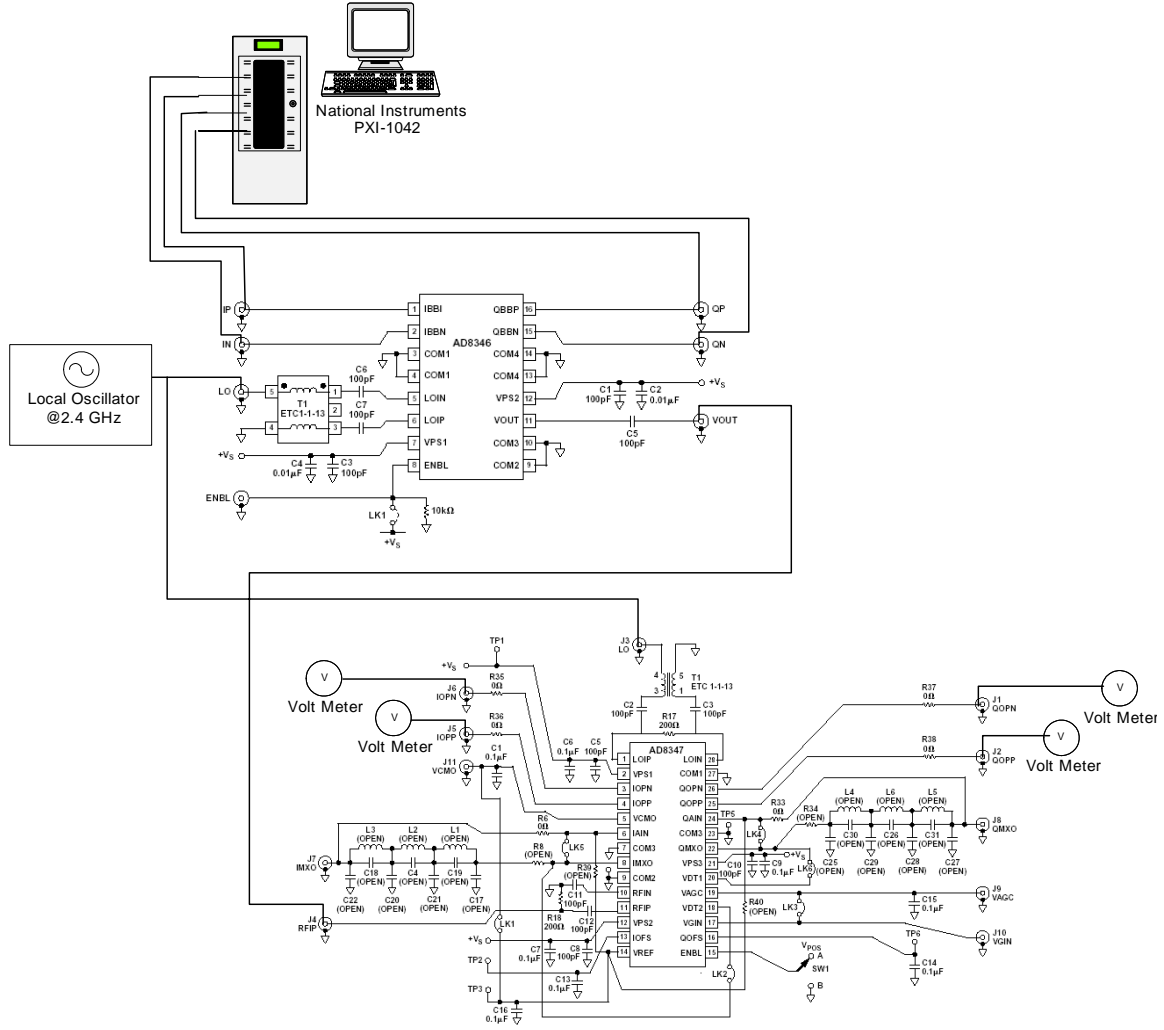


Figure 9. Experimental setup to measure the phase response of AD8347EVAL demodulator board (From Ref. [4].).

The RF signal output from one of the AD8346EVAL modulator boards is sent as the input to AD8347EVAL demodulator board. In this test setup, the LO carrier signal is set at 2.4 GHz and it is sent to both the modulator and demodulator. This is to ensure that the RF signal received by the AD8347EVAL demodulator can be downconverted to baseband signal with the same LO carrier signal used by AD8346EVAL modulator.

The connections on the AD8347EVAL board are shown in Figure 10. They include the dc power supply input VS, ground pin, LO signal input, RF signal input, VGIN, IOPN, IOPP, QOPN and QOPP. Both RF and LO signals connections are single-ended connections while IOPN, IOPP, QOPN and QOPP are differential connections. An external dc power supply is used to provide 5 VDC and proper grounding to VS and GNDs, respectively. The pin VGIN is used to control the gain of the RF and baseband variable gain amplifiers (VGA). The ON/OFF switch SW1 is used to enable and disable the external dc power supply to the board.

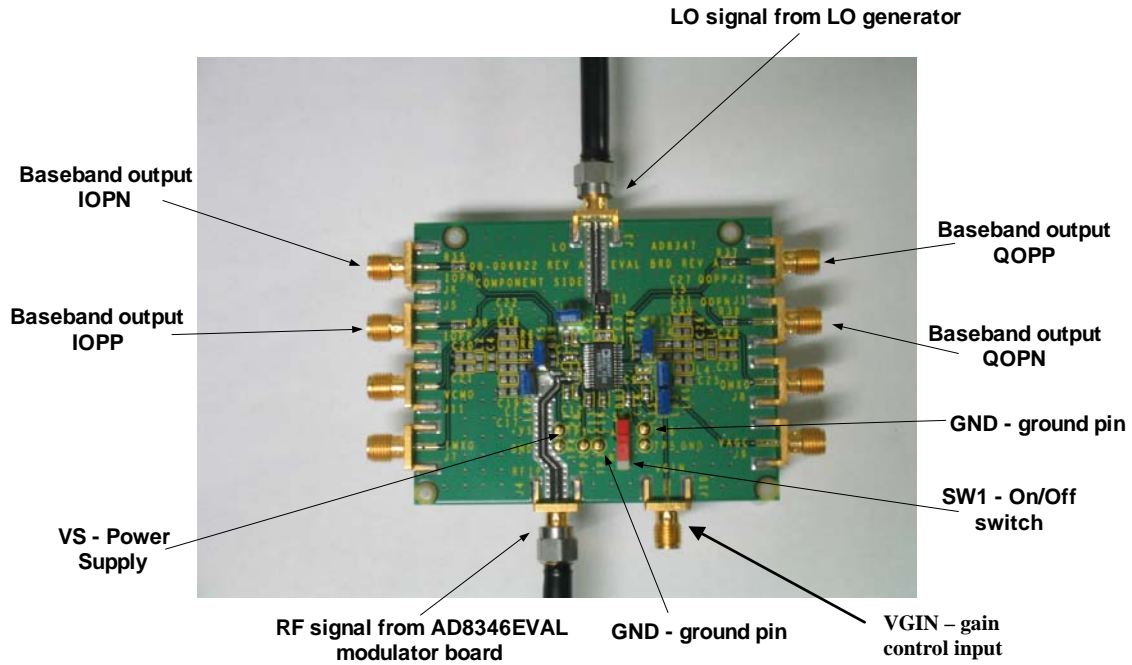


Figure 10. Signal connections to AD8347EVAL board (After Ref. [4].).

The specifications of AD8347 EVAL board [13] state that the operating range of the LO input level is between -10 to 0 dBm. Since the signal level supplied by the LO generator is 12 dBm, it is therefore necessary to lower the LO input level to -7 dBm by including a 19 dB RF attenuator in front of the LO input of the AD8347EVAL.

The amplitude and phase of the RF output signal from the transmit array is software programmable using a program written in LABVIEW. This RF signal is sent to the AD8347EVAL board where it is downconverted to quadrature baseband signals. The

voltage level of the quadrature baseband signals are obtained from the IOPN, IOPP, QOPN and QOPP, which are measured by using four digital multimeters.

3. Experimental Results

According to [13], the VGA gain needs to be connected to a external voltage source to improve the overall signal-to-noise ratio. This can be achieved by connecting VGIN to an external voltage source and turning off the AGC mode. The gain control voltage range of VGIN is between 0.2 and 1.2 V and hence 0.7 V is chosen to be the voltage level supplied by the external voltage source. This setup is slightly different from the one presented in [4]. In [4], the VGIN is in AGC mode where the gain is automatically adjusted until an internal threshold is met. Using the setup in [4] will result in phase errors, which are greatest near 45° , 135° , 225° and 315° phase shifts.

In this experiment, the phase of the RF signal was incremented by 10° steps starting from zero to 350° . The results from the in-phase and quadrature baseband signal outputs with 0.7 V supplied to VGIN and AGC mode being turned off are tabulated in Table 1.

Transmit Phase (in degrees)	IOPP (VDC) Voltage	IOPN (VDC) voltage	QOPP (VDC) Voltage	QOPN (VDC) voltage
0	1.0388	1.02442	0.99154	1.02121
10	0.98964	1.02559	0.99148	1.0213
20	0.98842	1.02679	0.99133	1.02141
30	0.98732	1.02784	0.99119	1.02158
40	0.98643	1.02884	0.99088	1.02189
50	0.98549	1.0298	0.99044	1.02231
60	0.98474	1.03058	0.98986	1.02293
70	0.98412	1.03113	0.98915	1.02365
80	0.98384	1.03153	0.98833	1.0245
90	0.98376	1.0316	0.98725	1.0255
100	0.98393	1.03141	0.9861	1.02673
110	0.98414	1.03121	0.98502	1.0278
120	0.9844	1.03104	0.98401	1.02883
130	0.98468	1.0306	0.98304	1.02982
140	0.98522	1.03013	0.98219	1.03068
150	0.98592	1.02943	0.98142	1.0314
160	0.98667	1.02865	0.98086	1.03199
170	0.98766	1.02768	0.98052	1.03229
180	0.98868	1.02667	0.98051	1.03234
190	0.98988	1.02544	0.9806	1.03228
200	0.99098	1.0243	0.9807	1.03212
210	0.99198	1.02324	0.98081	1.03189
220	0.99293	1.02223	0.98126	1.03157
230	0.99385	1.02137	0.98174	1.0311
240	0.9945	1.02067	0.98235	1.03046
250	0.99512	1.02013	0.9831	1.02977
260	0.9954	1.01983	0.9839	1.02891
270	0.99539	1.01984	0.985	1.02792
280	0.99523	1.01998	0.98617	1.0267
290	0.99502	1.02016	0.98726	1.02562
300	0.9948	1.02041	0.98833	1.02459
310	0.99435	1.02085	0.98926	1.02363
320	0.99396	1.02138	0.99014	1.02279
330	0.99333	1.02198	0.99089	1.02205
340	0.99253	1.02276	0.99147	1.02146
350	0.99176	1.02349	0.99182	1.02112

Table 1. Measurement results of AD8347EVAL Quadrature demodulator board.

Using the measurements of IOPP and IOPN, the differential voltages I were calculated by taking the difference between IOPP and IOPN. Similarly, this was also done for Q where the differences between QOPP and QOPN were used. After calculating the differential voltages, the received phase of the baseband signal was then calculated by using Equation (14).

Figure 11 shows a MATLAB plot for the measured differential I and Q components versus transmitted phase with VGIN is set to 0.7 V and AGC mode turned off. Cosine and sine waveforms are included in Figure 11 to compare with the measured in-phase and quadrature components. It is observed that the waveforms of the measured differential I and Q components are similar to the sinusoidal waveforms except for some amplitude scaling and a phase offset. This kind of phase offset is acceptable since it is present in all the other receive antenna elements. It is only the change in the phase difference between any 2 elements that will affect the receiver array output.

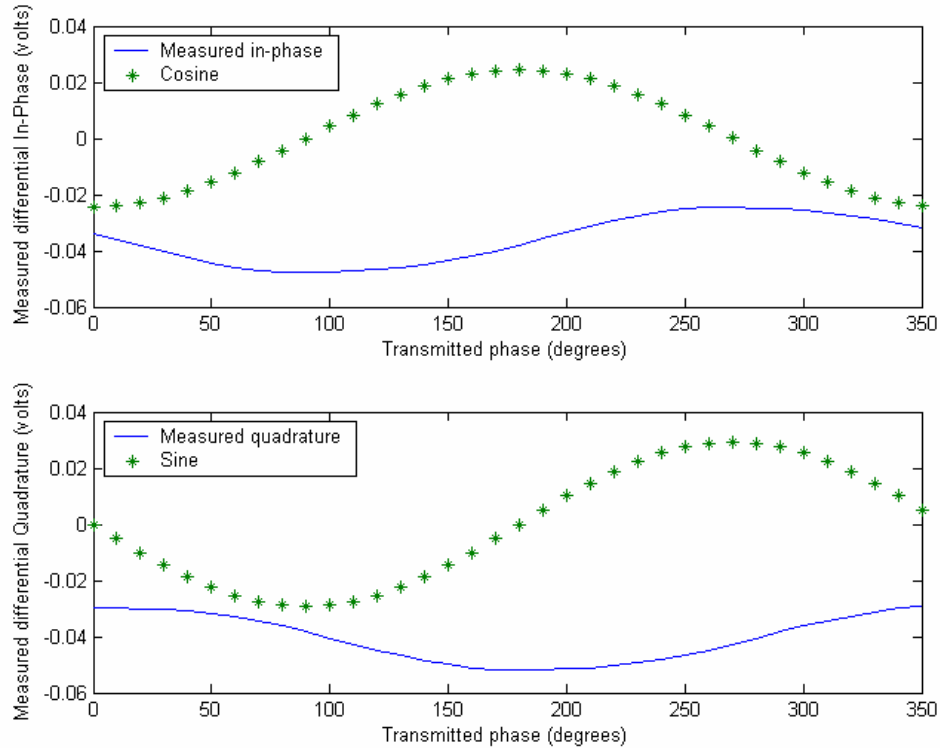


Figure 11. Measured differential I and Q components versus transmitted phase with VGIN set to 0.7 V and AGC mode turned off.

Figure 12 shows a plot of received phase versus transmitted phase with VGIN set to 0.7 V and AGC mode turned off. The values of the received phase and transmitted phase are very close and the slope of the received phase is always equal to +1. There are no visible ripples in the curves as compared with [4] where the ripples reached values as high as $\pm 20^\circ$. They were attributed to measurement errors and phase errors that occur in both the modulator and demodulator. The maximum phase errors that occurred at 45° , 135° , 225° and 315° reported [4] are no longer present as shown in Figure 12.

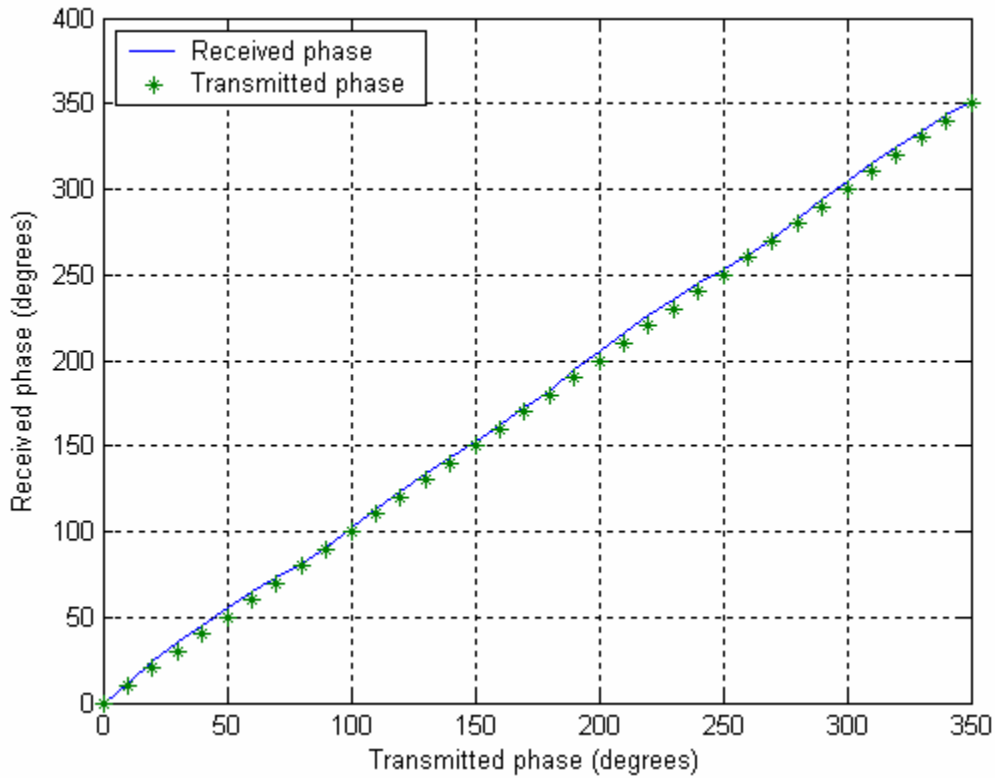


Figure 12. Received phase versus transmitted phase with VGIN set to 0.7 V and AGC mode turned off.

Figure 13 shows a plot of the phase error versus transmitted phase with VGIN set at 0.7 V and AGC mode turned off. This phase error is calculated by taking the difference of the received phase and transmitted phase as shown in Figure 12. The maximum phase error is about 6.5 degrees and it occurs when the transmitted phase is 220 degrees. The

calculated root mean square (RMS) phase error for this set of phase errors is 1.7881 degrees. Appendix B has more results on the phase response of the demodulator with AGC mode turned on.

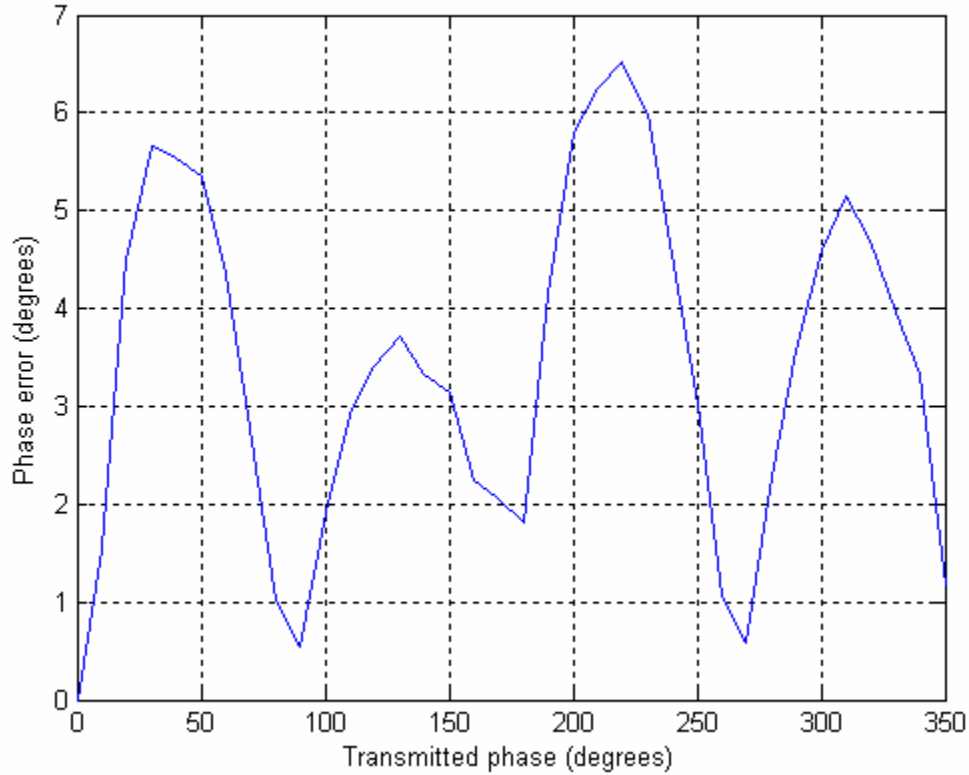


Figure 13. Phase error versus transmitted phase with VGIN set at 0.7 V and AGC mode turned off.

B. SIMULATION RESULTS USING TIME-VARYING PHASE WEIGHTS

LFM is one of the common signal waveforms used in radar applications. A technique of beam steering based on time-varying phase weights for LFM signals on transmit and receive is described in [5] and [6]. The benefits of using this technique are a reduction in the amount of phase distortion and an increase in the operating bandwidth of a linear array. In this section, the simulation results of a linear array transmitting a LFM waveform using different types of phase weights on transmit and receive is presented and discussed.

1. Preliminary Investigation of Using Time-varying Phase Weights on Transmit

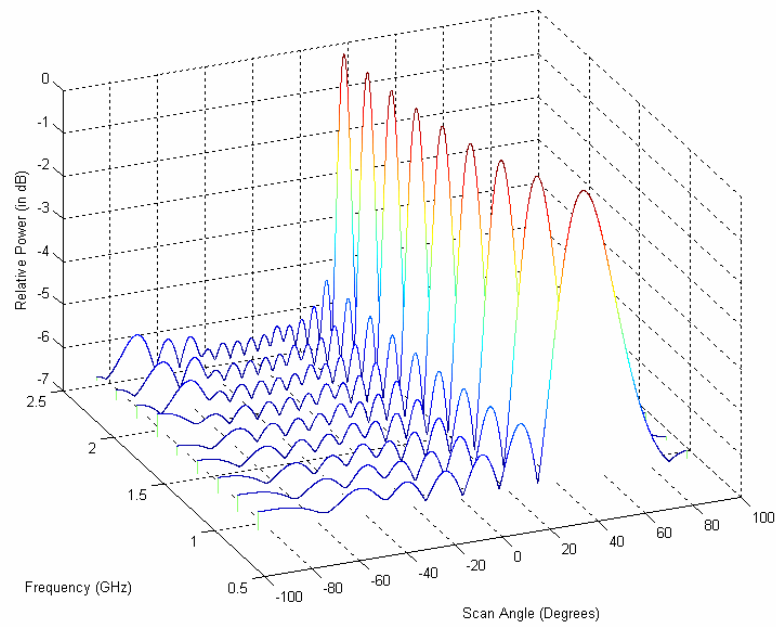
A simulation program was written to compare the wideband performance when fixed and time-varying phase weights are used on transmit for a sixteen-element linear phased array. In the simulation, the measured scattering parameter data (S_{21}) of the AD8346EVAL modulator board from [4] is used, where the magnitude of S_{21} in dB is the insertion loss and the phase of S_{21} is the insertion phase. The parameters used in this simulation are given in Table 2.

Parameters	Values
Reference frequency, f_r	1.7 GHz
Range of frequencies	0.8 to 2.4 GHz
Scan angle, θ	20°
Reference wavelength, λ_r	0.1765 m
Element spacing, d	0.08825 m

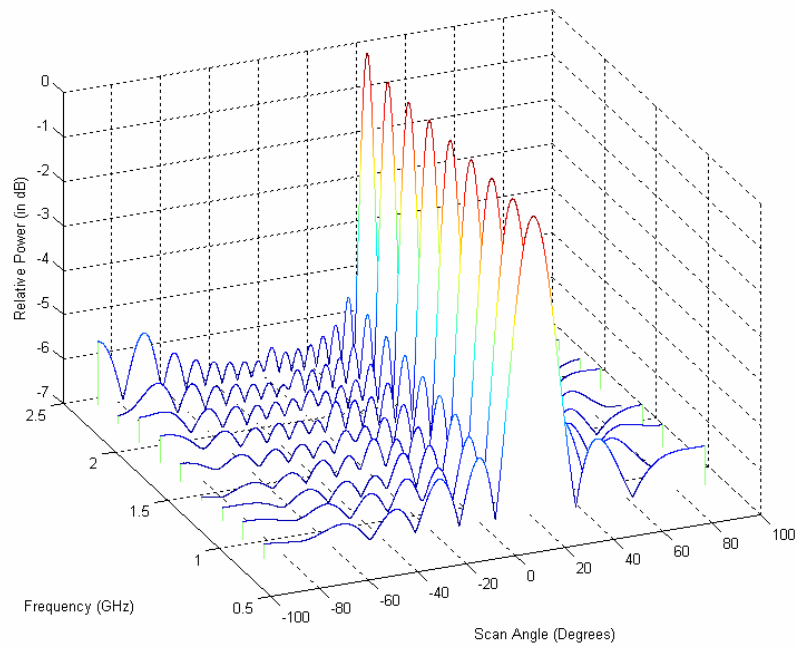
Table 2. Parameters used in simulation.

The reference frequency of 1.7 GHz was chosen because it is in the middle of the operating frequency range of the AD8346EVAL board. For this calculation, the element spacing was set equal to half the reference wavelength. The fixed phase weights were computed based on the reference frequency and remain constant over the range of frequencies. As for the time-varying phase weights, their values were computed based on the actual frequency that was being transmitted and, hence, vary over the range of frequencies.

Figure 14 shows two waterfall plots of the radiation patterns of a linear phased array using either constant or time-varying phase weights for transmit and receive. The parameters used for these plots are given in Table 2. For the case of using constant phase weights shown in Figure 14(a), the effects of beam squinting can be observed. In Figure 14(b), it is observed that the scan angle for a linear phased array using time-varying phase weights remains unchanged. However, the beamwidth of the main beam for both types of weights increases when the frequency of the signal is lower than the reference frequency, and decreases when the frequency of the signal is higher than the reference frequency.



(a) Using constant phase weights.



(b) Using time-varying phase weights.

Figure 14. Radiation patterns of a linear array using constant and time-varying phase weights.

2. Comparison of Phase Weighting Methods for LFM Signals

Figures 15, 16 and 17 show the matched filter output of LFM signal for a sixteen-element linear array. Three different types of phase weights on transmit and receive are shown for different scan angles. The three different types of phase weights used in this simulation are: (a) constant phase weights for both transmit and receive, (b) time-varying phase weights for transmit and constant phase weights for receive, and (c) time-varying phase weights for both transmit and receive. The fourth combination, constant phase weights for transmit and time-varying phase weights for receive, is not required, since by reciprocity, the result will be the same as the case of using time-varying phase weights for transmit and constant phase weights for receive.

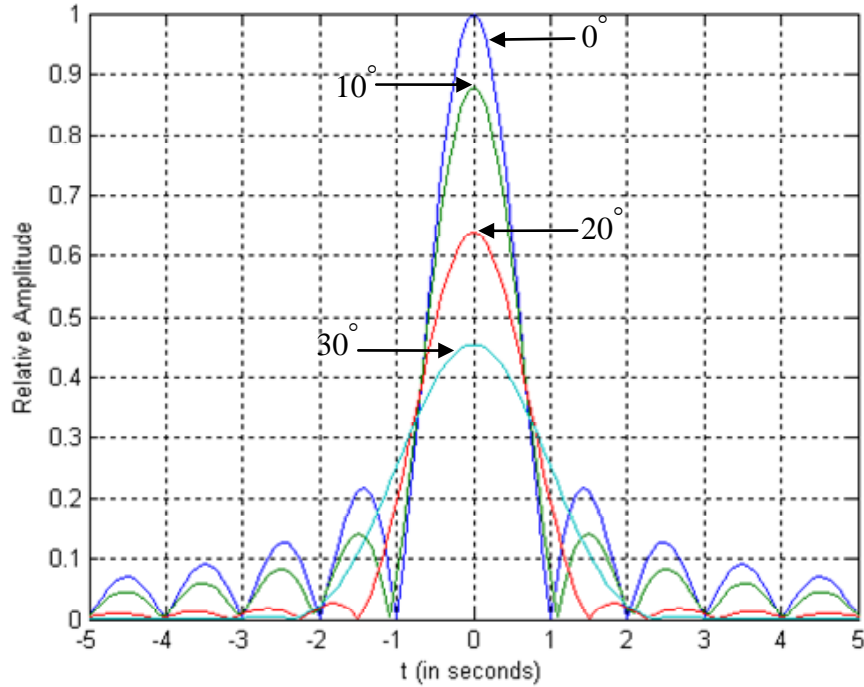


Figure 15. Matched filter output of LFM signal for 16-element linear array, $BT = 850$, with constant phase weights on transmit and receive, at different scan angles.

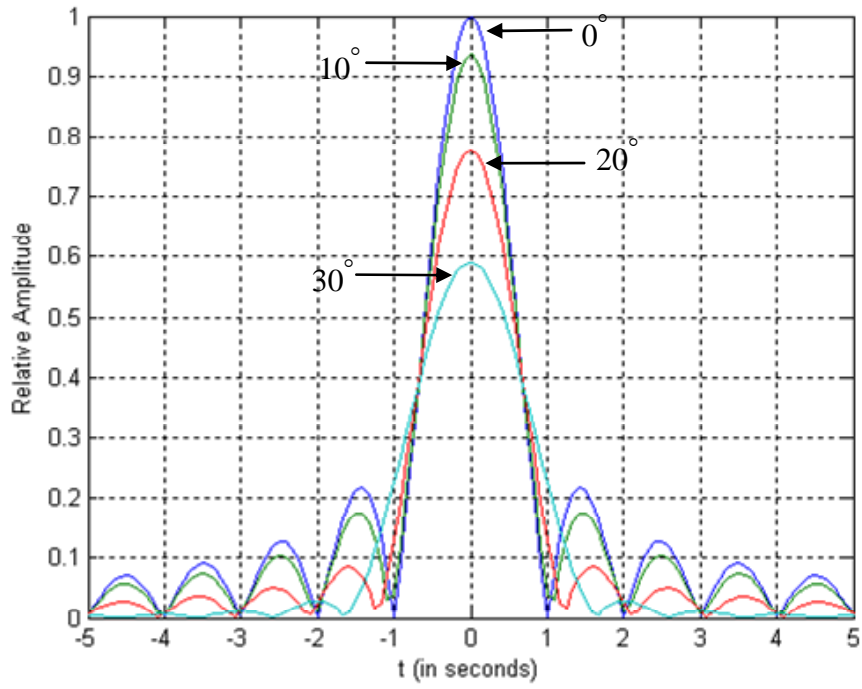


Figure 16. Matched filter output of LFM signal for 16-element linear array, $BT = 850$, with time-varying phase weights for transmit and constant phase weights for receive, at different scan angles.

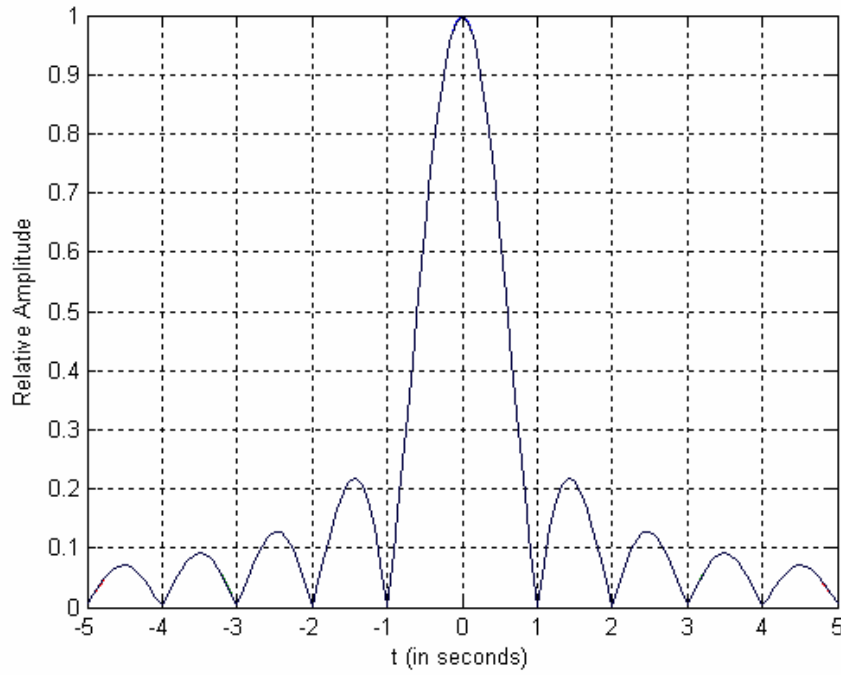


Figure 17. Matched filter output of LFM signal for 16-element linear array, $BT = 850$, with time-varying phase weights for both transmit and receive, at different scan angles.

The parameters used in this simulation are given in Table 3. The bandwidth was set to 50% of the reference frequency, and the element spacing set as a half the wavelength of the reference frequency. The time-bandwidth product used in this simulation is 850.

Parameters	Values
Number of array elements	16
Reference frequency, f_r	1.7 GHz
Reference wavelength, λ_r	0.1765 m
Element spacing, d	0.08825 m
Sweep period, T	1 μ s
Bandwidth, B	0.85 GHz
Time-bandwidth product, BT	850
Scan angles	0°, 10°, 20° and 30°

Table 3. Parameters used in the matched filter calculation for LFM signals.

From Figures 15 and 16, it is observed that in general, the beamwidth of the main lobes get broader and the relative amplitude decreases as the scan angle increases. In addition, the following observations are made by comparing Figures 15 and 16 at nonzero scan angles:

- The beamwidth of the main lobe in Figure 16 is not as broad as that shown in Figure 15.
- The relative amplitude of the main lobe in Figure 16 is higher than that in Figure 15.

In Figure 17, the matched filter output is the same regardless of the scan angle. The beamwidth of the main lobe and the relative amplitude of the matched filter output are the same for all scan angles.

In summary, using time-varying phase weights on transmit improves the matched filter output performance relative to using constant phase weights. In applications where the range of the target is known *in priori*, then using time-varying phase weights for both transmit and receive provides the best performance.

Next, the effect of the time-bandwidth product on the performance of the matched filter output was investigated. The value of the bandwidth stated in Table 3 was increased to 1.36 GHz which results in a new time-bandwidth of 1360. The simulation results of the matched filter output with the new time-bandwidth product are shown in Figures 18 and 19. In Figures 18 and 19, at the scan angle of 30 degrees, the beamwidth of the main lobe is broader in Figure 19 than in 18. This result indicates that when the time-bandwidth product is large and a narrow beamwidth of the main lobe is desired, the technique of using time-varying phase weights on transmit is effective for small scan angles.

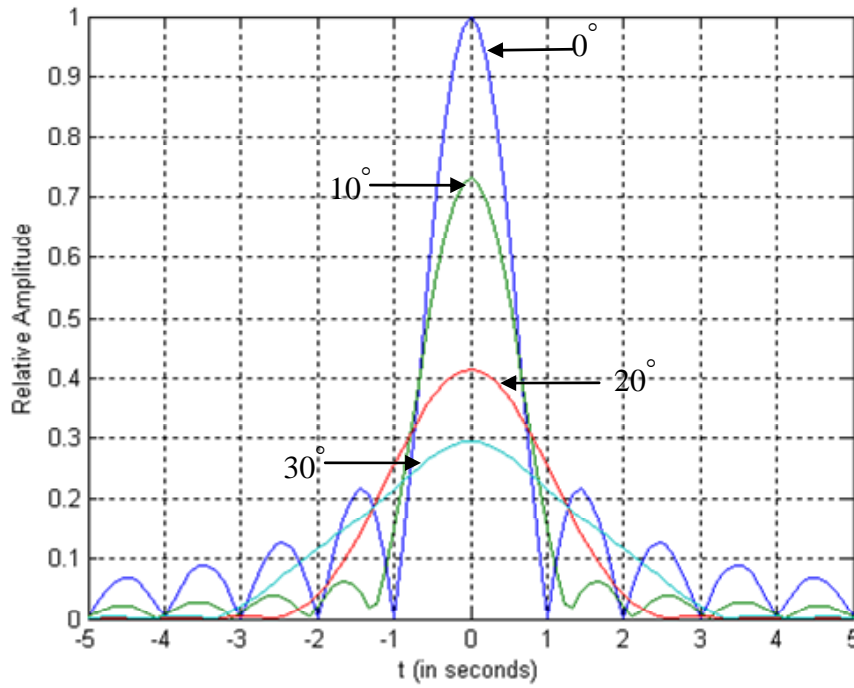


Figure 18. Matched filter output of LFM signal for 16-element linear array, $BT = 1360$, with constant phase weights both transmit and receive, at different scan angles.

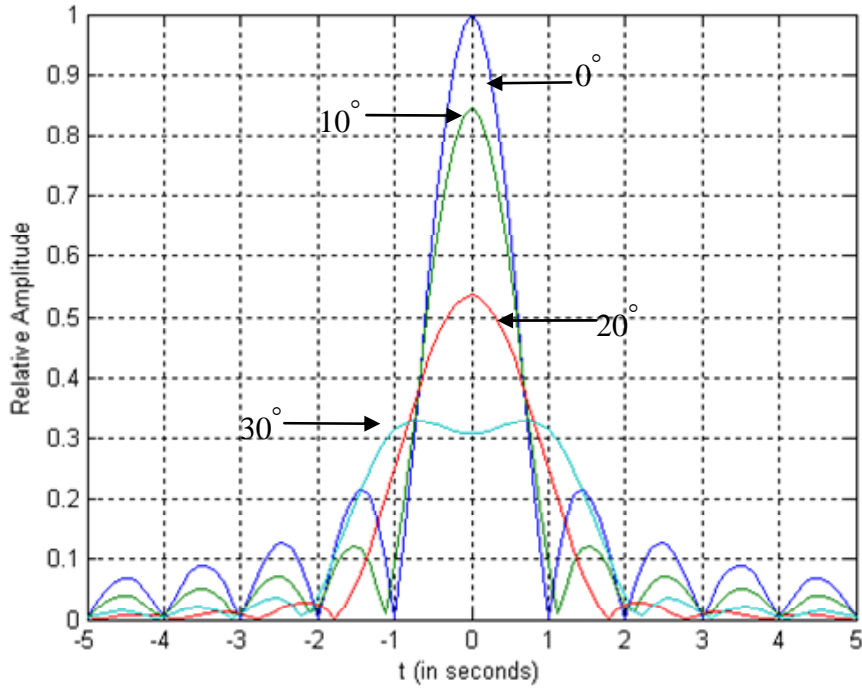


Figure 19. Matched filter output of LFM signal for sixteen-element linear array, $BT = 1360$, with time-varying phase weights on transmit and constant phase weights on receive at different scan angles.

3. Loss in Signal-to-Noise Ratio (SNR) Comparison for Different Types of Phase Weights

Using the same parameters as shown in Table 3, and by varying the scan angle and bandwidth, the loss of SNR when different types of phase weights are used on transmit and receive are simulated. The range of the scan angles used in this simulation is from 0° to 60° at increments of 10° . The bandwidth percentage in the figure is computed with respect to the center frequency. The results are shown in Figure 20. One observation is that the loss of SNR increases with increasing bandwidth and scan angle. The loss in SNR, for the case where time-varying phase weights are used on transmit and constant phase weights are used on receive, is also lower than using constant phase weights on both transmit and receive. Also, by reciprocity, having time-varying phase weights on either transmit or receive improves the SNR performance.

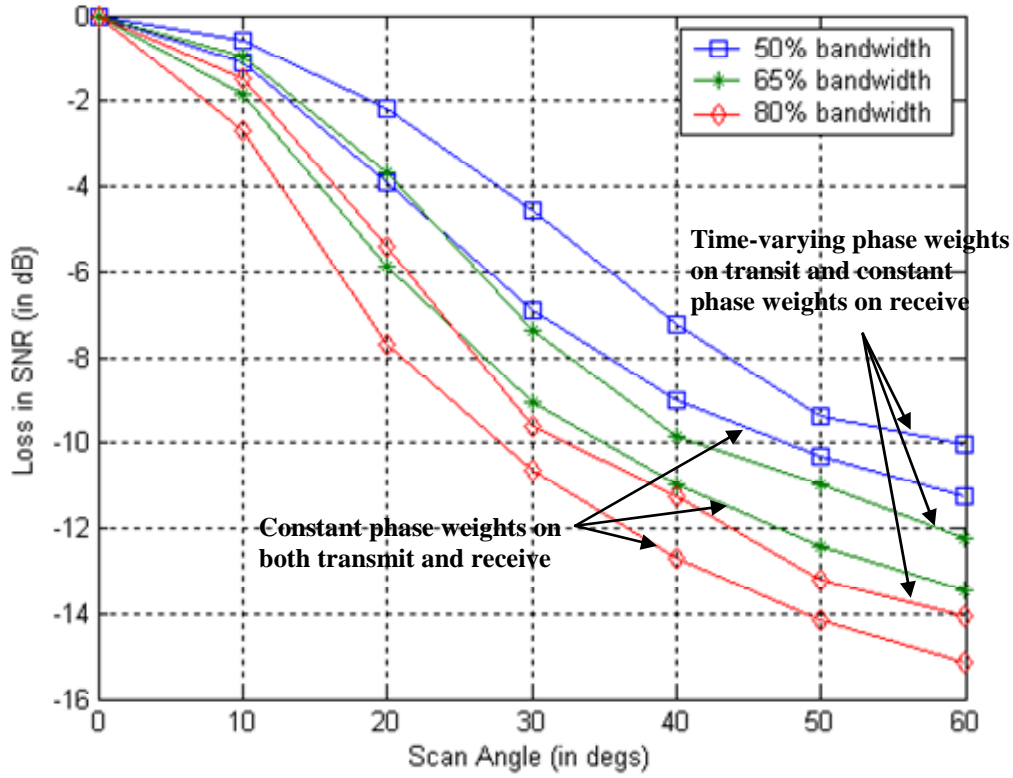


Figure 20. Comparison of loss in SNR between using time-varying phase weights and constant phase weights for receive, and constant phase weights for both transmit and receive.

C. APPROACH TO IMPLEMENT TIME-VARYING PHASE WEIGHTS ON TRANSMIT USING COTS COMPONENTS

In this section, the approach to implement time-varying phase weights in a sixteen-element linear transmit phased array, with single sideband (SSB) LFM signals using COTS components is discussed. Details of the COTS components are provided, and some preliminary experimental results for the implementation are also provided.

1. Laboratory Setup for Transmit Architecture

Direct digital synthesis technology has advanced rapidly, but direct synthesis of ultra-high frequency (UHF) and microwave frequencies is still not economically feasible. A DDS is normally integrated with a phase locked loop (PLL) or a mixer for upconversion. The method of multiplication with PLLs affects the signal integrity, frequency reso-

lution and agility. By using a mixer to upconvert a double sideband (DSB) signal to SSB requires difficult filtering and also a high quality LO. There are methods to reduce these undesired effects but they will require multiple PLLs or multiple stages of mixer/filter/-oscillator.

In [14], a single stage quadrature implementation of a SSB upconverter using a AD9854 DDS and a AD8346 modulator was demonstrated. It was shown in [14] that the upconverted SSB signal is capable of greater than 36-dB typical rejection of LO and other sideband signals without compromising the signal qualities. This 36-dB rejection capability is adequate to satisfy most communication applications requirements. It also helps to reduce the filtering requirement and, hence, reduce cost and complexity of the filter. Figure 21 shows a block diagram using the AD9854 DDS and AD8346 modulator to generate a upconverted SSB to the LO frequency with 36 dB typical SSB rejection. It is possible to set the desired SSB signal at either upper or lower sidebands. This can be done by exchanging the cables of the quadrature DDS output signals, from I to Q and Q to I , that send data to the AD8346.

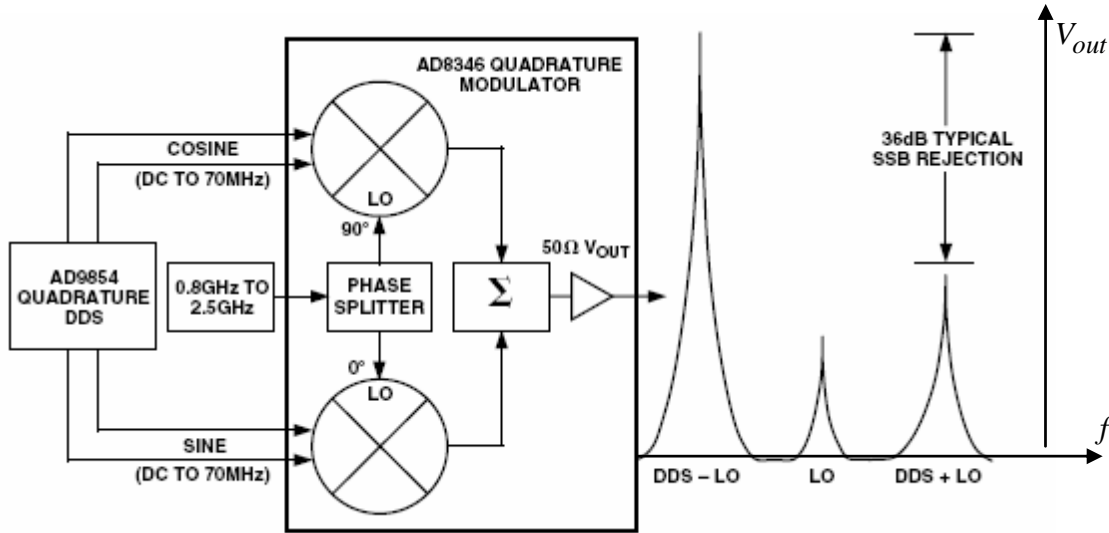


Figure 21. Quadrature DDS SSB upconversion using AD9854 and AD8346 (From Ref. [14].).

The laboratory setup to demonstrate the upconversion of the quadrature DDS SSB was configured as shown in Figure 22 to implement the time-varying phase weights for a sixteen-element linear transmit phased array.

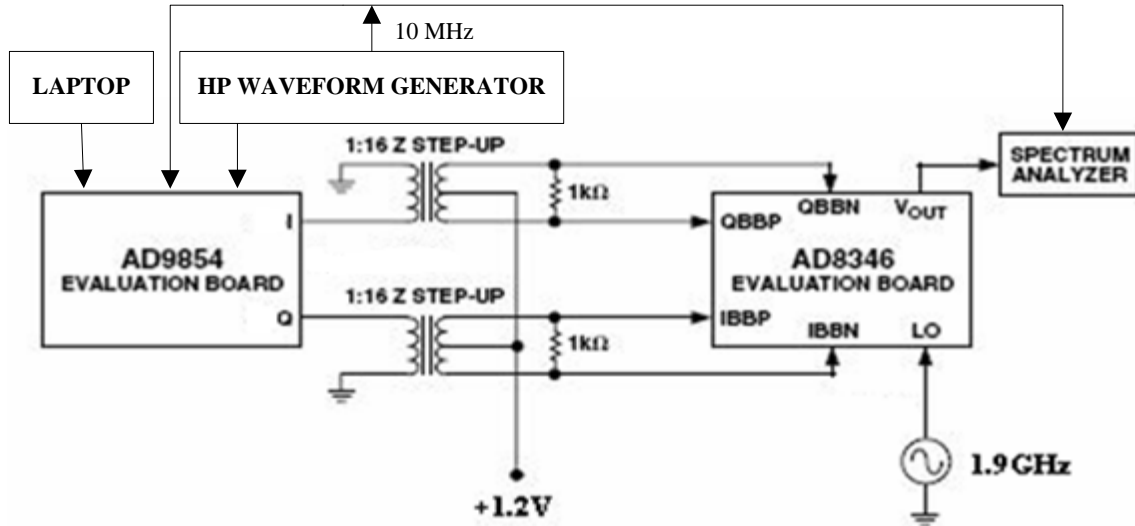


Figure 22. Laboratory setup for SSB upconversion (After Ref. [14].).

Since the output I and Q signals from AD9854EVAL are single-ended, and the output voltage level is inadequate to meet the input requirements of the AD8346EVAL, a center-tapped impedance step up transformer was required to provide differential outputs to AD8346EVAL and increase the voltage levels for both the I and Q outputs from the AD9854EVAL. The AD9854EVAL evaluation software (version 1.72) was installed onto a laptop and used to program the generation of LFM signals from the AD9854-EVAL board. A laptop was connected to the AD9854EVAL board via the parallel port, and a waveform generator used to provide the clock required by the AD9854EVAL board.

a. *AD9854EVAL Direct Digital Synthesizer*

The AD9854EVAL digital synthesizer board is a highly integrated device that uses advanced DDS technology to form a digitally programmable I and Q synthesizer function. It is able to provide a 48-bit programmable frequency resolution from 1 μHz to 300 MHz. It also has dual 14-bit programmable phase offset registers to control the phase from 0 to 360 degrees. Modulation techniques such as frequency shift keying (FSK), binary phase shift keying (BPSK), phase shift keying (PSK), CHIRP and amplitude modulation (AM) can also be generated. The CHIRP mode in AD9854EVAL supports both a linear and non-linear FM sweep patterns, and it can be used for wide band-

width frequency sweeping applications. It allows accurate and internally generated LFM over a specific frequency range, duration, frequency resolution and sweep direction. Hence, the AD9854EVAL is chosen to generate the LFM signals and is also used to set the time-varying phase weights given in Equations (7) and (8).

Figure 23 shows a block diagram of the AD9854EVAL DDS board. The AD9854EVAL architecture allows the generation of simultaneous quadrature output signals at frequencies up to 150 MHz. It provides two 14-bit phase registers and two 12-bit I and Q DACs which provides excellent wideband and narrowband output spurious-free dynamic range (SFDR). The programmable multiplier circuit (4 to 20 times REFCLK) is capable of generating the 300-MHz system clock internally from a lower frequency external reference clock.

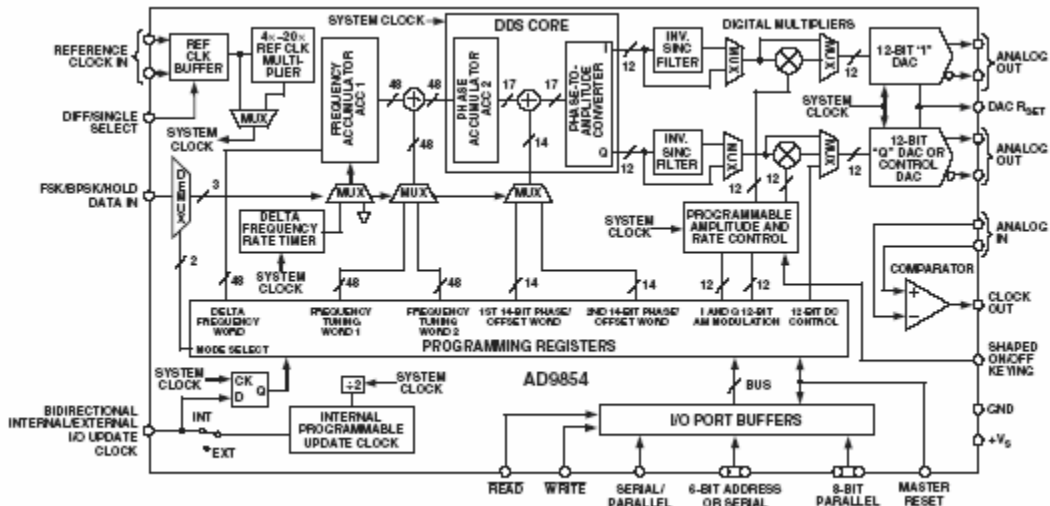


Figure 23. Block diagram of AD9854 DDS (From Ref. [15].).

Figure 24 shows a view of the AD9854EVAL evaluation software (revision 1.72) graphic user interface (GUI) for generating LFM signals. The first step is to select the Chirp Mode at the top of the screen and program the start frequency into Frequency Tuning Word #1 either in binary or real number. Next, the frequency step resolution, range from 1 Hz to 200 MHz, is programmed into the 48-bit, two's complement Frequency Step Word. The most significant bit (MSB) of this Frequency Step Word defined the slope of the frequency in the LFM. If the MSB is 1, then the frequency is decreasing

incrementally from the start frequency. If it is 0, then the frequency is increasing incrementally from start frequency. The time spent on each frequency can be programmed by using the equation given by [15]

$$(N + 1) \times (\text{system clock period}) \quad (14)$$

where N is the 20-bit Frequency Step Rate Counter value and the system clock period is set to 5 ns. Phase Adjust #1 is a 14-bit output phase offset that affects both the I and Q outputs of the AD9854EVAL. The phase offset term in Equation (7) was programmed into the Phase Adjust #1 and the frequency term in Equation (8) was programmed into the Frequency Step Word.

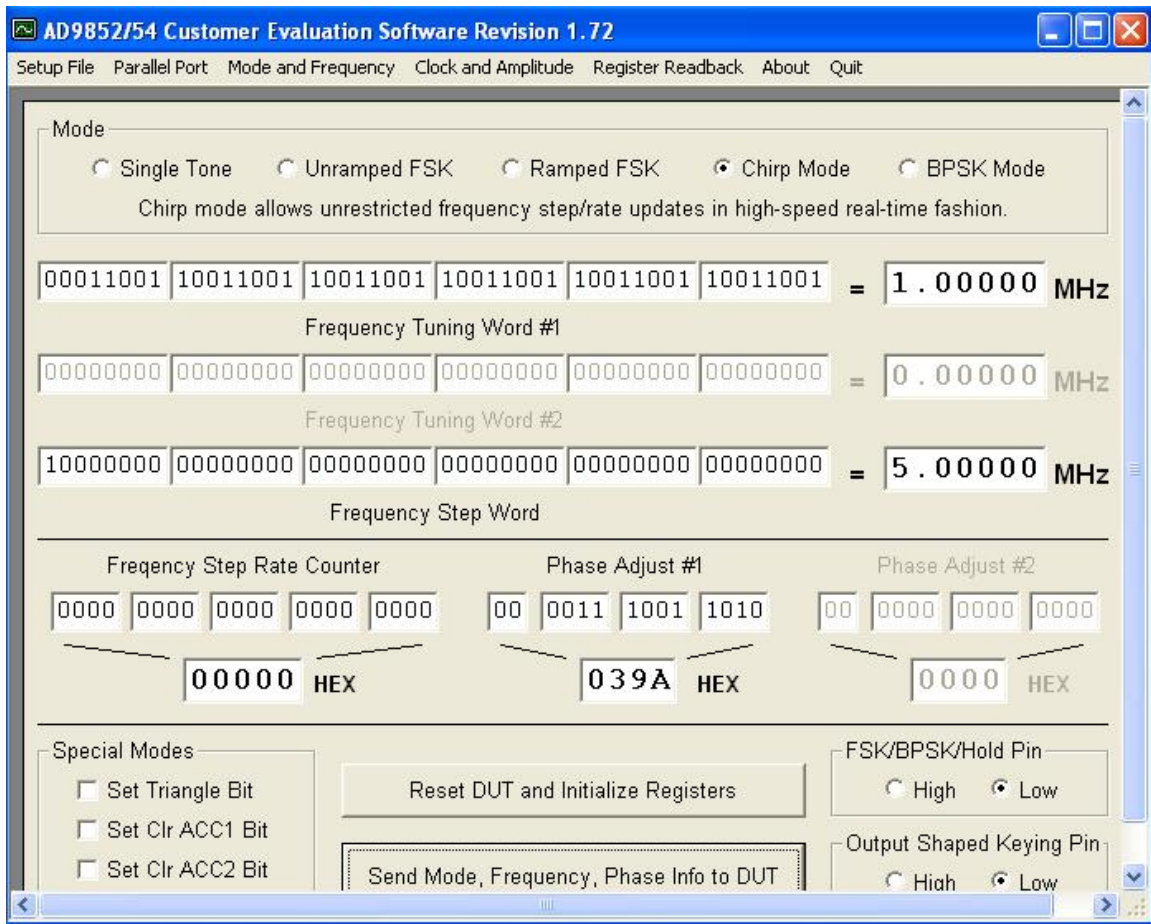


Figure 24. AD9854EVAL evaluation software (version 1.72) GUI.

Figure 25 shows the cable and signal connections of AD9854EVAL board to other equipment used in the setup shown in Figure 23. The laptop that was used to con-

trol the AD9854EVAL board was connected to it via the parallel input port. A 10-MHz signal from a waveform generator was provided to the single-ended clock input (J25) on the board. The terminal block 1 (TB1) on the board consists of AVDD, DVDD, VCC and GND pins, and the voltage being supplied to AVDD, DVDD and VCC is 3.3 V. The AVDD supplied the voltage to all the devices under test (DUT) analog pins while the DVDD supplied voltage to all the DUT digital pins. The VCC supplied voltage to all other devices that are not being covered by AVDD and DVDD. The GND pin, which was connected to the ground of the external power supply, provided grounding to all the devices on the AD9854EVAL board. The quadrature output signals from the AD9854-EVAL board were obtained at J6 (Filtered IOUT) and J7 (Filtered IOUT2), respectively, which were then connected to the step up transformer.

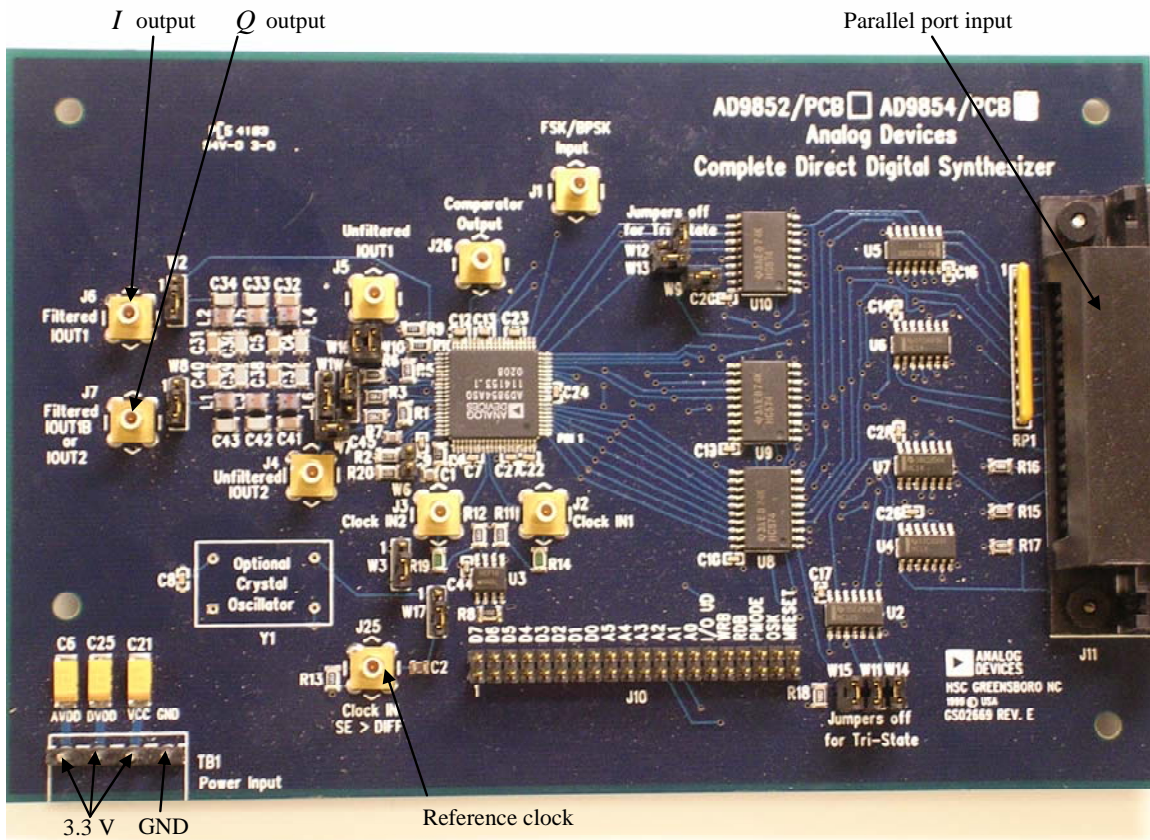


Figure 25. AD9854EVAL cable and signal connections.

b. Fabrication of Step-up Transformer

One reason for having the 1:16 center-tapped impedance step-up transformers between AD9854EVAL and AD8346EVAL was to increase the I and Q output voltage level of 1 V peak to peak to the required voltage level for IBBN, IBBP, QBBN and QBBP input signals of AD8346EVAL, which is 2 V peak to peak. Another reason is to create four differential input signals for AD8346EVAL since the quadrature output signals from AD9854EVAL are signal-ended. A voltage level of 1.2 V was provided to the center-tapped secondary windings to comply with input bias requirement for AD8346EVAL differential input signals.

Figure 26 shows the schematic diagram of a center-tapped impedance step-up transformer. The step-up transformer is a RF transformer (T16-6T) from Mini-circuits with frequency range from 0.03 to 75 MHz.

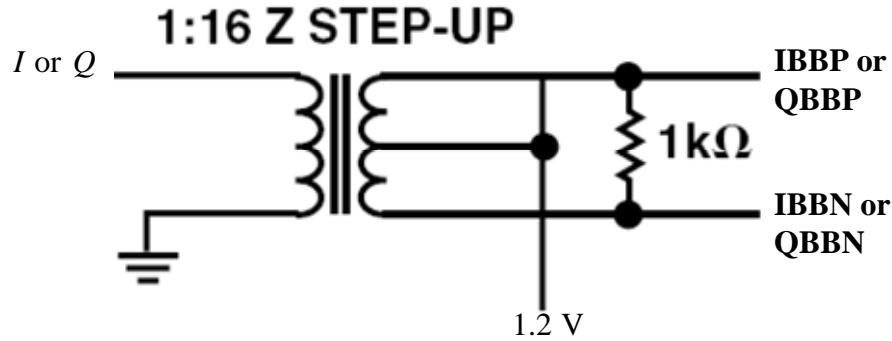


Figure 26. Schematic diagram of center-tapped impedance step-up transformer (After Ref. [14].).

A printed circuit board (PCB) for the step-up transformer was designed based on the schematic diagram shown in Figure 26. The PCB was designed using a software tool, Easily Applicable Graphical Layout Editor (EAGLE) Version 4.13 for Windows (Light Edition). A Mathcad program found in [16] was used to calculate the required trace width to ensure that the impedance is 50 ohms. The parameters used in the design of the microstrip transmission lines using PCB laminates are given in Table 4. The PCB was fabricated by Electronic Controls Design Inc. and the material used is FR-4, the standard glass epoxy substrate. Figure 27 shows that PCB board diagram of the

step-up transformer with two subminiature version A (SMA) connectors for the quadrature output signals from AD9854EVAL, and four SMA connectors for the IBBN, IBBP, QBBN and QBBP input signals of the AD8346EVAL.

Parameters	Values
Dielectric thickness	0.062 "
Dielectric constant (for FR4)	4.81
Copper weight	1 oz
Thickness of copper	0.00135 "
Thickness of plated copper	0.014 "
Trace width	0.105 "

Table 4. Parameters used in the design of microstrip transmission line.

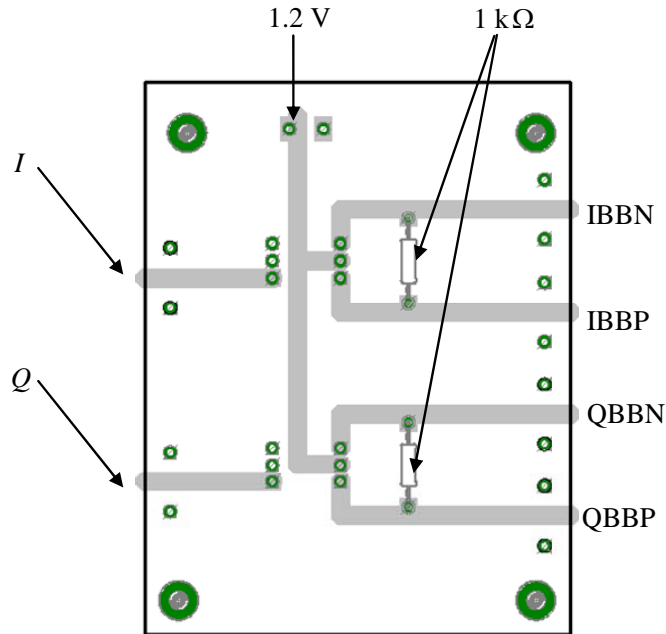


Figure 27. Board diagram for the step up transformer.

2. Preliminary Results

In order to measure the frequency spectrum of the AD8346, the LO frequency was set equal to 1.9 GHz and the clock frequency was set to 100 kHz. The frequency

range of the LFM signal was programmed to be from 10 to 15 MHz. The parameters stated in Table 5 were programmed into the AD9854EVAL software and the measured frequency spectrum output of the AD8346EVAL is shown in Figure 28. The spectrum analyzer used was a Hewlett-Packard (HP) Spectrum Analyzer, model number 8562A.

Parameters	Values
Frequency step rate counter	0.001
Frequency step word	0.025 MHz
Frequency Tuning Word #1	10 MHz
Phase Adjust #1	0

Table 5. Parameters used for Figure 28.

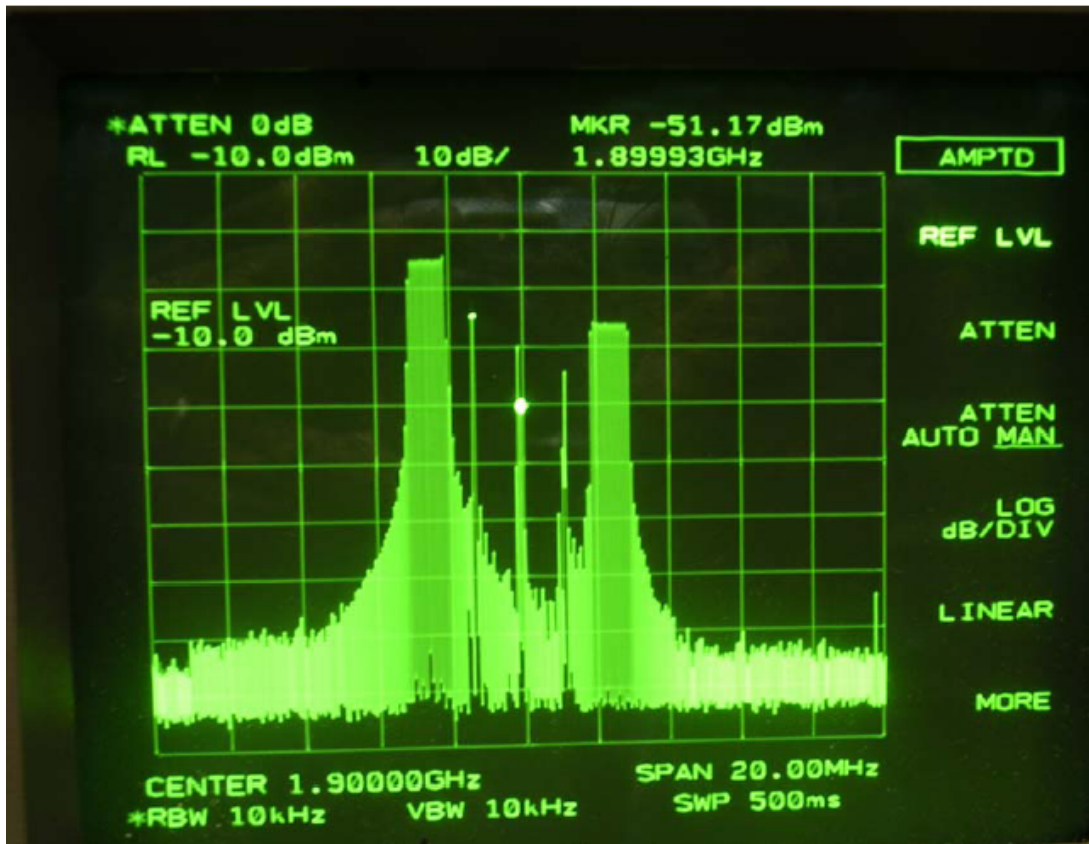


Figure 28. Frequency spectrum output of AD8346EVAL at center frequency equal to 1.9 GHz.

Another result is provided in Figure 29 where the center frequency used in this figure was 2.1 GHz and the clock frequency was set to 100 kHz. The frequency range of the LFM signal was programmed to be from 2 to 3 MHz. The other parameters required by the AD9854EVAL software are given in Table 6. The frequency spectrum output of the AD8346EVAL using the parameters in Table 6 is shown in Figure 29.



Figure 29. Frequency spectrum output of AD8346EVAL at center frequency equal to 2.1 GHz.

Parameters	Values
Frequency step rate counter	0.001
Frequency step word	0.005 MHz
Frequency Tuning Word #1	2 MHz
Phase Adjust #1	0

Table 6. Parameters used for Figure 29.

As shown in both Figures 28 and 29, the difference in the two sidebands is about 10 dB and not the 36-dB as expected in [14]. This level of suppression is inadequate and hence bandpass filtering is required to remove the insufficiently suppressed sideband at the output of AD8346EVAL. This inadequacy of suppression could be due to the quadrature phase errors and amplitude imbalance within AD9854EVAL and AD8346EVAL. Another possible cause of error is the use of external components such as the step transformers, unequal cable length and PCB. Any slight difference in the performance of the two step transformers can result in different amplitude levels for the quadrature signals; whereas unequal cable length can cause phase errors. Note that the phase errors that occur within AD9854EVAL and AD8346EVAL cannot be corrected. However, the phase errors caused by unequal cable lengths can be corrected simply by using equal cables for the connections between AD9854EVAL and AD8346EVAL.

a. Simulation Result of I and Q Phase and Amplitude Imbalance

One of the possible causes of the inadequate suppression of one of the sidebands is the I and Q phase and amplitude imbalance. The typical I and Q amplitude and phase imbalance for AD9854EVAL are about 0.15 dB and 0.2 degree, respectively. For the AD8346EVAL, the typical I and Q amplitude and phase imbalance are 0.2 dB and 1 degree, respectively.

Figure 30 shows the results of a simulation where the worst case of the AD9854EVAL I and Q amplitude and phase imbalance of 0.5 dB and 1 degree are introduced to a LFM signal. The parameters used for the generation of the LFM signal are a sweep period of 1 μ s, signal bandwidth of 10 MHz, center frequency of 20 MHz and LO frequency of 1.9 GHz. In Figure 30, an image SSB signal was generated due to the I and Q amplitude and phase imbalance. The difference between the two SSB signals is about 22 dB and this was only due to the AD9854EVAL. If the effect of another error source such as AD8346EVAL was to be included, the difference between the two SSB signals will decrease further.

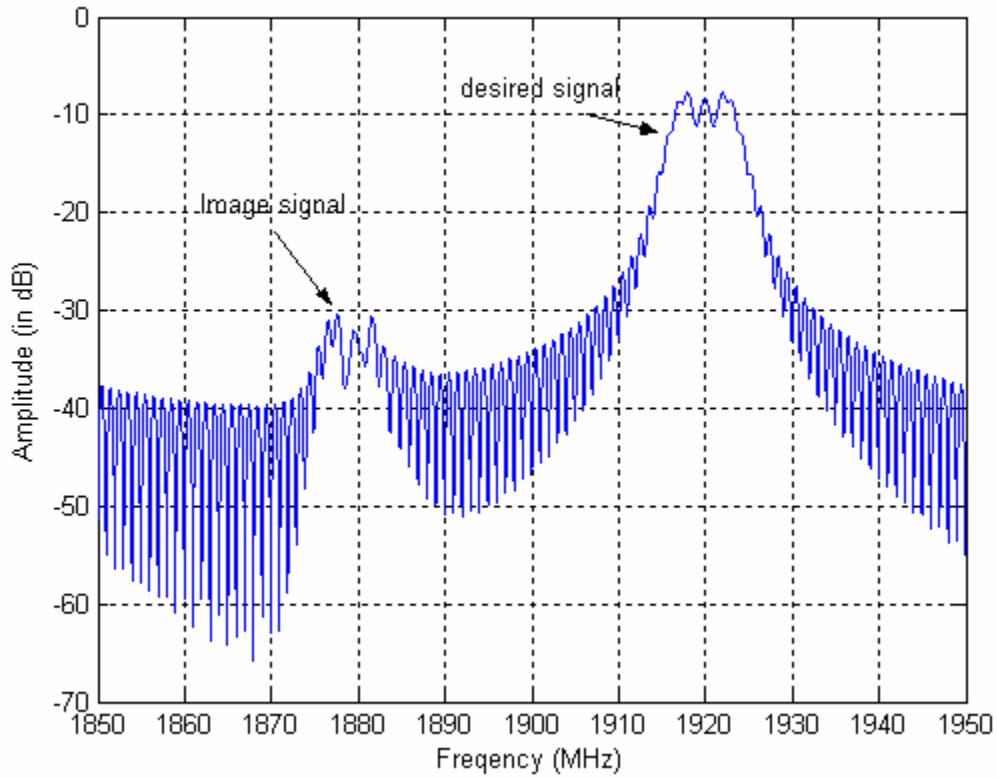


Figure 30. Effect of I and Q amplitude and phase imbalance.

3. Future Work

In order to demonstrate the performance of LFM signals using time-varying phase weights on transmit and constant phase weights on receive, it is necessary to remove the undesired sideband as shown earlier. This can be achieved by inserting a bandpass filter at the output of the AD8346EVAL modulator. One potential candidate for the bandpass filter is a 3G transmit bandpass filter (Model no: WSF-00154) from K & L Microwave. The passband of this filter is from 2110 to 2170 MHz with a rejection of at least 60 dB for 0 to 2090 MHz and 50 dB for 2190 to 4000 MHz. It also has low passband insertion loss of 1 dB maximum.

The proposed experimental setup to verify the performance of using time-varying phase weights on transmit and constant phase weights on receive is given in Figure 31. This setup consists of only one antenna element out of the sixteen-element linear phased array. For a particular scan angle, the time-varying phase weights for each of the antenna elements on the transmit side are programmed one at a time using the laptop before all

are sent to the AD9854EVAL board. At the AD8346EVAL board, the baseband signal is upconverted to a RF signal and sent as the input to AD8347EVAL board. This input signal is then downconverted to I and Q baseband components by mixing with the LO signal. The I and Q voltage outputs are measured at the pins IOPP, IOPN, QOPP and QOPN of the AD8347EVAL board. In order to simulate a sixteen-element phased array, this process needs to be repeated sixteen times. With these measurements after some signal processing, the matched filter output for the sum of the sixteen-element quadrature signal outputs is then compared with the theoretical improvement. Due to the tight schedule of this research, the results for this proposed experimental setup were not collected.

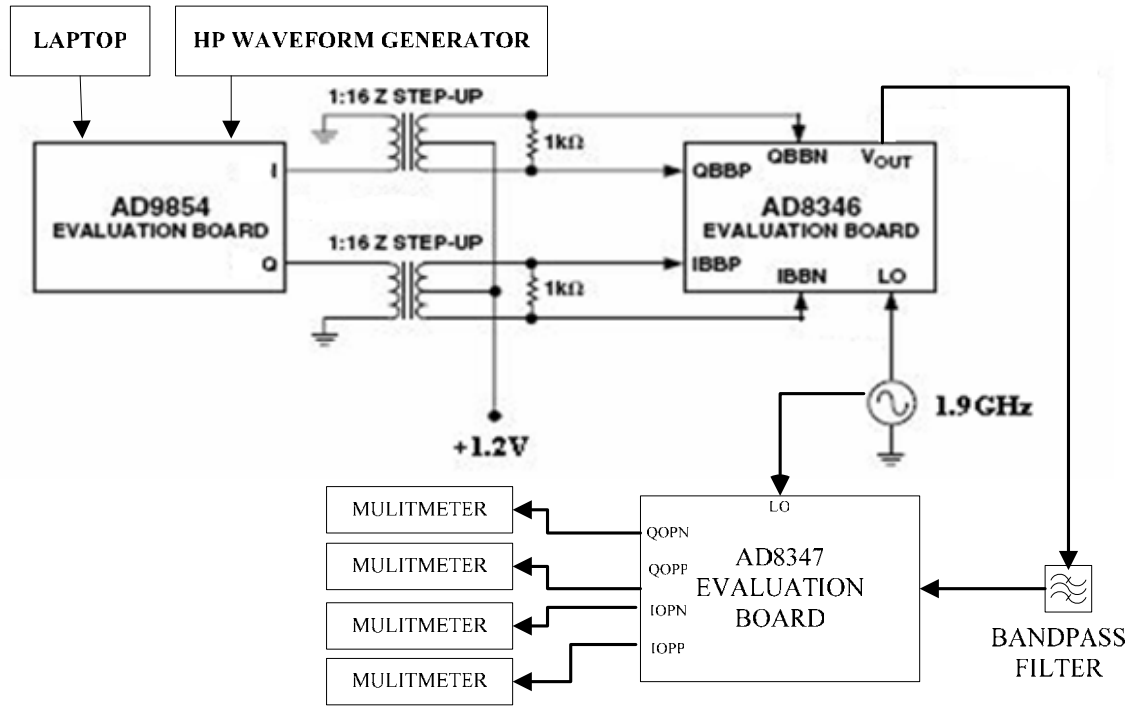


Figure 31. Proposed experimental setup for time-varying phase weights on transmit and constant phase weights on receive.

D. SUMMARY

In the first part of this chapter, the measured phase response of AD8347EVAL demodulator with VGIN set at 0.7 V and AGC mode turned off was presented. The phase response result shows that the maximum errors at 45°, 135°, 225° and 315° reported previously are no longer present, and the difference between the received phase and transmitted phase is acceptably small.

Next, the simulation results of the matched filter output for a LFM signal when different types of time-varying phase weights were used on transmit and receive, was presented and discussed. It was shown that using time-varying phase weights on both transmit and receive has the best performance, but this required that the range of the target to be known *a priori*. The more practical way is to use either time-varying phase weights on transmit or receive, and constant phase weights on the other. It was shown that using time-varying phase weights on transmit improved the relative amplitude and decreased the broadening of the beam as the scan angle increased. However, as the time-bandwidth product increased, the technique of using time-varying phase weights on transmit was only effective for small scan angles. The loss in SNR performance was also investigated and it was found that using time-varying phase weights on transmit improved the loss in SNR performance as compared to using constant phase weights.

The approach to implement time-varying phase weights on transmit using COTS components was discussed. A preliminary laboratory setup using a AD9854EVAL DDS and AD8346EVAL board to implement time-varying phase weights on transmit was shown and results were presented. The details of the COTS components that were used in this experiment were also provided. From the preliminary results, it was found that the AD8346EVAL was not able to suppress the image signal by 36 dB and hence a bandpass filter is required. Some details on the work that needs to be done was also provided.

IV. CONCLUSIONS AND FUTURE WORK

A. CONCLUSIONS

Phased array systems play an important role in both military and civilian applications. The design of such a system is typically complex and requires a large number of specially designed and integrated components. It is therefore beneficial to leverage on the low cost and high performance COTS components for the building of such a system.

Further investigation of the periodic phase error mentioned in [4] revealed that this error arose due to inappropriate operating conditions of the commercial AD8347-EVAL demodulator and was not caused by the commercial AD8346EVAL modulator. The results of the phase response of a AD8347EVAL demodulator, with VGIN set at 0.7 V and AGC mode turned off, showed that the phase difference between the received and transmitted phase is small, and there were no large errors at 45° , 135° , 225° and 315° , as previously reported in [4].

In order to improve the phase distortion and increase the operating bandwidth of the phased array, a technique of using different types of time-varying phase weights for a LFM signal on both transmit and receive was investigated. The simulation results showed that using time-varying phase weights on both transmit and receive achieved the best performance, but this method required the range of the target to be known *a priori*. It is more practical to use time-varying phase weights on only one side (either transmit or receive, but not both), and constant phase weights on the other side. Having time-varying phase weights on transmit, as the scan angle increases, helps to improve the relative amplitude of the matched filter output and decrease the broadening of the filter response. The results also show that this technique is only effective for small scan angles when the time-bandwidth is high. The SNR performance was also investigated and the results showed that the SNR performance improved by using time-varying phase weights.

A preliminary laboratory setup using COTS components was presented to implement the time-varying phase weights on the transmit side. The COTS components include a AD9854EVAL DDS and a AD8346EVAL demodulator board. The results

showed that AD8346EVAL was not able to provide a suppression of 36 dB on the image signal and hence a bandpass filter is required.

B. SUGGESTIONS FOR FUTURE WORK

1. Implement Time-varying Phase Weights on the Transmit Side

The next step in this research is to continue the implementation of the time-varying phase weights on the transmit side using COTS components. With the bandpass filter and the laboratory setup as described in Chapter III, the data collected can be used to compute the matched filter output which will be used to compare with the simulation results.

2. Arrays Transmit and Receive Antenna with Time Delay Units

In order for the phased array antenna to achieve wideband performance, a time-delay architecture is required for the transmit and receive antenna. In the process of introducing digital TDUs into the phased array systems, it is important to understand the effects of TDU quantization errors in a wideband phased array system. In [17], it was shown that the quantization errors from TDUs cause time delay offsets between subarrays and result in a loss of both SNR and range resolution.

3. Time Delay Beam-steering

Analog TDUs, which are costly and bulky, are normally used as the time delay beam-steering in phased array systems. A method is described in [18] that avoids the use of analog TDUs to implement time delay beam-steering without introducing range-dependent losses. This method is an extension to the stretch processing technique and employs only low-speed digital sampling and signal processing. Future work can be done to implement this method using suitable COTS components.

APPENDIX A: MATLAB CODES

% This Matlab code is used to simulate Array factor of a N element linear array

```
clear all
close all

j=sqrt(-1);
c=3e08;           % speed of light
fc=1.7e9;         % carrier frequency
lamda1= c/fc;     % wavelength
d=0.5*lamda1;     % element spacing = half wavelength
k1=2*pi/lamda1;   % propagation constant for signal at original frequency
N=16;            % number of elements
theta0 = 30;      % initial steer angle in degrees, measured from the array axis
increment=pi/10000; % increment of scan angle

theta=-pi/2:increment:pi/2; % scan from -pi/2 to pi/2
theta0= deg2rad(theta0);    % to convert from degrees to radians

sum1=0;
for n=0:N-1
    value1 = exp(j*(n*k1*d*(sin(theta)-sin(theta0))));
    sum1 = sum1 + value1;
end
AF1=sum1/max(sum1); %normalised AF

figure(1)
plot(rad2deg(theta),20*log10(AF1),'k');
axis([-90 90 -50 0])
grid
ylabel('Relative power (dB)')
xlabel('\theta (degrees)')
```

% This Matlab code is to simulate Array factor of a N element linear array at 3 different frequencies

```
clear all
close all
j=sqrt(-1);
c=3e08;           % speed of light
fc=1.7e9;         % carrier frequency
lamda1= c/fc;     % wavelength
d=0.5*lamda1;     % element spacing = half wavelength
lamda2=c/0.8e9;
lamda3=c/2.5e9;
k1=2*pi/lamda1;   % propagation constant for signal at original frequency
k2=2*pi/lamda2;   % propagation constant for signal at lower frequency
k3=2*pi/lamda3;   % propagation constant for signal at higher frequency
N=16;            % number of elements
theta0 = 20;      % initial steer angle in degrees, measured from the array axis
increment=pi/10000; % increment of scan angle

theta=-pi/2:increment:pi/2; % scan from -pi/2 to pi/2
theta0= deg2rad(theta0);    % to convert from degrees to radians

sum1=0;
sum2=0;
sum3=0;
```

```

for n=0:N-1
    value1 = exp(j*(n*k1*d*(sin(theta)-sin(theta0))));
    newtheta1 = asin(k1/k2*sin(theta0));
    value2 = exp(j*(n*k2*d*(sin(theta)-sin(newtheta1))));
    newtheta2 = asin(k1/k3*sin(theta0));
    value3 = exp(j*(n*k2*d*(sin(theta)-sin(newtheta2))));
    sum1 = sum1 + value1;
    sum2 = sum2 + value2;
    sum3 = sum3 + value3;
end

tempmax= max(max(sum1),max(sum2));
maxsum=max(tempmax, max(sum3));
AF1=sum1/maxsum; %normalised AF
AF2=sum2/maxsum; %normalised AF
AF3=sum3/maxsum; %normalised AF

figure(1)
plot(rad2deg(theta),20*log10(AF1),'k',rad2deg(theta),10*log(AF2),'-r',rad2deg(theta),10*log(AF3),'-g');
axis([-90 90 -30 0])
ylabel('Relative power (dB)')
xlabel('\theta (degrees)')
legend('freq = 1.7GHz','freq = 0.8GHz','freq = 2.5GHz',2)

```

% This Matlab code is used to plot the graph to show the phase response of AD8347EVAL with and without VGIN set at 0.7V

```

clear
close all
sgn = 1;
ss = csvread('Measured 8347 17 Jul AGC 0.7V demodulator board 1.csv');

%read data
IP = ss(:,2);
IN = ss(:,3);
QP = ss(:,4);
QN = ss(:,5);

I = IP-IN;
Q = QP-QN;
I1 = I-mean(I);
Q1 = Q-mean(Q);

I1 = I1;          %/max(I1);
Q1 = Q1;          %/max(Q1);
ang = sgn*rad2deg(unwrap(atan2(Q1,I1)));

xaxis = 0:10:350;

A =max(I)*(cos(xaxis*pi/180));
B =max(Q)*(sin(xaxis*pi/180));

figure(1);
xaxis = 0:10:350;
subplot(211); plot(xaxis,IP,xaxis,IN);
ylabel('Voltage')
subplot(212); plot(xaxis,QP,xaxis,QN)
ylabel('Voltage')

figure(2);
xaxis = 0:10:350;

```

```

plot(xaxis,ang-min(ang),xaxis,xaxis,'*')
max(ang)-min(ang)
xlabel('Transmitted phase (degrees)'); ylabel('Received phase (degrees)')
legend('Received phase','Transmitted phase',2)
grid

figure(3);
xaxis = 0:10:350;
plot(xaxis,ang-min(ang)-xaxis.);
rms = std(ang-min(ang)-xaxis.)
xlabel('Transmitted phase (degrees)'); ylabel('Phase error (degrees)')
grid

figure(4);
subplot(211);
plot(xaxis, I, xaxis, A, '*');
xlabel('Transmitted phase (degrees)'); ylabel('Measured differential In-Phase (volts)')
legend('Measured in-phase','Cosine',2)
subplot(212);
plot(xaxis, Q, xaxis, B, '*');
xlabel('Transmitted phase (degrees)'); ylabel('Measured differential Quadrature (volts)')
legend('Measured quadrature','Sine',2)

```

% A Matlab code to generates the waterfall plot of Pattern Factor as a function of reference frequency.
 % Uses the S21 values measured from the modulator.

```

c = 3e8;
reffreq = 1.7e9;
lamda= c/reffreq;

noofElements = 16;
ScanAngle = 20;
d = lamda/2;
n = (0:noofElements-1).';
load s21raw

faxis = linspace(0.8,2.5,201).';
fchoice = (-0.9:0.2:0.8) + (reffreq/1e9);
theta = -90:0.05:90;
AFt = zeros(length(theta),length(fchoice));
AFt1 = zeros(length(theta),length(fchoice));

for kk = 1:length(fchoice)
    angle = (2*pi*fchoice(kk)*1e9/c)*d*n*sin(deg2rad(ScanAngle)); % Plumb's method
    angle2 = (2*pi*reffreq/c)*d*n*sin(deg2rad(ScanAngle)); % Conventional method
    angle1 = round(rad2deg(mod(angle,2*pi)));
    angle3 = round(rad2deg(mod(angle2,2*pi)));
    s21 = zeros(noofElements-1,1);
    s211 = zeros(noofElements-1,1);
    AF1 = [];
    AF2 = [];
    for ii = 0:noofElements-1;
        s21(ii+1) = interp1(faxis,raw(:,angle1(ii+1)+1),reffreq/1e9);
        s211(ii+1) = interp1(faxis,raw(:,angle3(ii+1)+1),reffreq/1e9);
    end
    for jj = theta
        AF1 = [AF1 sum(s21.*exp(-j*2*pi*fchoice(kk)*1e9/c*d*n*sin(deg2rad(jj))))];
        AF2 = [AF2 sum(s211.*exp(-j*2*pi*fchoice(kk)*1e9/c*d*n*sin(deg2rad(jj))))];
    end
    AFt(:,kk) = AF1.';
    AFt1(:,kk) = AF2.';
end

```

end

```
figure(1)
[U,V]=meshgrid(theta,fchoice);
hold on
waterfall(U,V,(abs(AFt1.))-max(max(abs(AFt))))))
ylabel('Frequency (GHz)')
xlabel('Scan Angle (Degrees)')
zlabel('Relative Power (in dB)')
view([-23 34])
```

```
figure (2)
waterfall(U,V,(abs(AFt1.))-max(max(abs(AFt))))))
ylabel('Frequency (GHz)')
xlabel('Scan Angle (Degrees)')
zlabel('Relative Power (in dB)')
view([-23 34])
```

% A Matlab code to plot the matched filter for 16-element linear array with constant phase weights on transmit and
% receive

```
% LFM waveform parameters
c = 3e8;
B = 0.5*1.7e9; % Bandwidth LFM
T = 1e-6; % Sweep Period
fo = 1.7e9;
lamda = c/fo; % Center frequency
mu = B/T;
fs = 4*(B+fo); % Sampling frequency
ts = 1/fs;
t = (-T/2:ts:T/2-ts).';
lent = length(t);
d = lamda/2; % Element spacing

% Array parameters
N = 16; % number of elements
M = deg2rad(0:10:60); % Target Angles (theta_t)
lenM = length(M);
thetat = max(M);
ft = exp(j*2*pi*(fo*t+mu/2*(t.^2)));
maxDelayCells= round(2*(N-1)/c*d*sin(thetat)/ts); % Maximum delay across array from edge to edge
if mod(maxDelayCells,2) ~= 0, maxDelayCells = maxDelayCells + 1; end

maxln = length(t)+ maxDelayCells;
tref = linspace(0,(ts*(maxln-1)),maxln).';
t = linspace(-maxln*ts/2,maxln*ts/2,maxln).';
maxt2 = 2*max(t);
win = [zeros(maxDelayCells/2,1); ones(size(ft)); zeros(maxDelayCells/2,1)];
ft = [zeros(maxDelayCells/2,1); ft; zeros(maxDelayCells/2,1)];
lenft = length(ft);
cumstore = zeros(length(t),lenM);
dum = N-1;
for kk = 1:lenM
    tmp4 = zeros(maxln,1);
    for pp = 0:N-1
        for qq = 0:N-1
            tmp0 = round((pp+qq-dum)/c*d*sin(M(kk))/ts);
            ncell = wshift('1D',win,tmp0);
            tmp1 = exp(j*pi*mu*((pp+qq-dum)*d*sin(M(kk))/c).^2);
            tmp2 = exp(-j*2*pi*(pp+qq-dum)*d/c*(mu*t*sin(M(kk))));
            tmp4 = tmp4 + tmp1.*tmp2.*ncell;
```

```

        end
    end
    cumstore(:,kk) = tmp4.*ft;
    disp(kk)
end

outarray = cumstore/N/N;
ax = linspace(0,length(outarray)-1,length(outarray));
tmp = zeros(size(outarray,1)*2-1,4);
xx = abs(xcorr(outarray(:,1),(ft))*ts);
tmp(:,1) = xx;
mtmp = max(tmp(:,1));
tmp(:,1) = tmp(:,1)/mtmp;
tmp(:,2) = abs(xcorr(outarray(:,2),(ft))*ts)/mtmp;
tmp(:,3) = abs(xcorr(outarray(:,3),(ft))*ts)/mtmp;
tmp(:,4) = abs(xcorr(outarray(:,4),(ft))*ts)/mtmp;

P = 4;
figure(1);
for ii = 1:P
    subplot(P,1,ii);
    plot(ax,real(outarray(:,ii)));
end

ax1 = linspace(-length(tmp)/2,length(tmp)/2,length(tmp));
ax1 = ax1*ts*B;
figure(2);
for ii = 1:P
    subplot(P,1,ii);
    plot(ax1,tmp(:,ii));
end

figure(3);
plot(ax1,tmp(:,1),ax1,tmp(:,2),ax1,tmp(:,3),ax1,tmp(:,4))
xlabel('t (in seconds)');
ylabel('Relative Amplitude');
grid
axis([-5 5 0 1])

```

% A Matlab code to plot the matched filter for 16-element linear array with time-varying phase weights on transmit
% and constant phase weights on receive

```

% LFM waveform parameters
c = 3e8;
B = 0.8*1.7e9;           % Bandwidth LFM
T = 1e-6;                % Sweep period
fo = 1.7e9; lamda = c/fo;
mu = B/T;
fs = 4*(B+fo);           % Sampling frequency
ts = 1/fs;
t = (-T/2:ts:T/2-ts).';
lent = length(t);
d = lamda/2;             % Separation of array elements

% Array parameters
N = 16;                  % Number of elements
M = deg2rad(0:10:60);
lenM = length(M);
thetat = max(M);
ft = exp(j*2*pi*(fo*t+mu/2*(t.^2)));
maxDelayCells= round(2*(N-1)/c*d*sin(thetat)/ts);

```

```

if mod(maxDelayCells,2) ~= 0, maxDelayCells = maxDelayCells + 1; end

maxln = length(t)+ maxDelayCells;
tref = linspace(0,(ts*(maxln-1)),maxln).';
t = linspace(-maxln*ts/2,maxln*ts/2,maxln).';
maxt2 = 2*max(t);
win = [zeros(maxDelayCells/2,1); ones(size(ft)); zeros(maxDelayCells/2,1)];
ft = [zeros(maxDelayCells/2,1); ft; zeros(maxDelayCells/2,1)];

lenft = length(ft);
cumstore = zeros(length(t),lenM);
dum = (N-1)/2;
for kk = 1:lenM
    tmp4 = zeros(maxln,1);
    for pp = 0:N-1
        for qq = 0:N-1
            tmp0 = round((pp+qq-dum)/c*d*sin(M(kk))/ts);
            ncell = wshift('1D',win,tmp0);
            tmp1 = exp(j*pi*mu*((qq-dum)*d*sin(M(kk))/c).^2);
            tmp2 = exp(-j*2*pi*(qq-dum)*d/c*(mu*t*sin(M(kk))));
            tmp4 = tmp4 + tmp1.*tmp2.*ncell;
        end
    end
    cumstore(:,kk) = tmp4.*ft;
end

outarray = cumstore/N/N;
ax = linspace(0,length(outarray)-1,length(outarray));
tmp = zeros(size(outarray,1)*2-1,4);
xx = abs(xcorr(outarray(:,1),(ft))*ts);
tmp(:,1) = xx;
mtmp = max(tmp(:,1));
tmp(:,1) = tmp(:,1)/mtmp;

tmp(:,2) = abs(xcorr(outarray(:,2),(ft))*ts)/mtmp;
tmp(:,3) = abs(xcorr(outarray(:,3),(ft))*ts)/mtmp;
tmp(:,4) = abs(xcorr(outarray(:,4),(ft))*ts)/mtmp;

P = 4;

figure(1);
for ii = 1:P
    subplot(P,1,ii);
    plot(ax,real(outarray(:,ii)));
end

ax1 = linspace(-length(tmp)/2,length(tmp)/2,length(tmp));
ax1 = ax1*ts*B;

figure(2);
for ii = 1:P
    subplot(P,1,ii);
    plot(ax1,tmp(:,ii));
end

figure(3);
for ii = 1:P
    plot(ax1,tmp(:,P)); hold on
end
hold off
plot(ax1,tmp(:,1),ax1,tmp(:,2),ax1,tmp(:,3),ax1,tmp(:,4))

```



```

xlabel('t (in seconds)');
ylabel('Relative Amplitude');
axis([-5 5 0 1])
grid

```

% A Matlab code to plot the matched filter for 16-element linear array with time-varying phase weights on transmit
% and receive

```

% LFM waveform parameters
c = 3e8;
B = 0.5*1.7e9; % Bandwidth LFM
T = 1e-6; % Sweep period
fo = 1.7e9;
lamda = c/fo; % Center frequency
mu = B/T;
fs = 4*(B+fo); % Sampling frequency
ts = 1/fs;
t = (-T/2:ts:T/2-ts).';
lent = length(t);
d = lamda/2; % element spacing

% Array parameters
N = 16; % number of elements
M = deg2rad(0:10:60); % Target Angles (theta_t)
lenM = length(M);
thetat = max(M);
ft = exp(j*2*pi*(fo*t+mu/2*(t.^2)));
maxDelayCells = round(2*(N-1)/c*d*sin(thetat)/ts);
if mod(maxDelayCells,2) ~= 0, maxDelayCells = maxDelayCells + 1; end
maxln = length(t) + maxDelayCells;
tref = linspace(0,(ts*(maxln-1)),maxln).';
t = linspace(-maxln*ts/2,maxln*ts/2,maxln).';
maxt2 = 2*max(t);
win = [zeros(maxDelayCells/2,1); ones(size(ft)); zeros(maxDelayCells/2,1)];
ft = [zeros(maxDelayCells/2,1); ft; zeros(maxDelayCells/2,1)];
%ft = [ft; zeros(maxDelayCells,1)];
lenft = length(ft);
cumstore = zeros(length(t),lenM);
dum = N-1;
for kk = 1:lenM
    tmp4 = zeros(maxln,1);
    for pp = 0:N-1
        for qq = 0:N-1
            tmp0 = round((pp+qq-dum)/c*d*sin(M(kk))/ts);
            ncell = wshift('1D',win,tmp0);
            tmp1 = exp(0); % n+k = pp+qq-dum
            tmp2 = exp(0);
            tmp4 = tmp4 + tmp1.*tmp2.*ncell;
        end
    end
    cumstore(:,kk) = tmp4.*ft;
    disp(kk)
end

outarray = cumstore/N/N;
ax = linspace(0,length(outarray)-1,length(outarray));
tmp = zeros(size(outarray,1)*2-1,4);
xx = abs(xcorr(outarray(:,1),(ft))*ts);
tmp(:,1) = xx;
mtmp = max(tmp(:,1));
tmp(:,1) = tmp(:,1)/mtmp;

```

```

tmp(:,2) = abs(xcorr(outarray(:,2),(ft))*ts)/mtmp;
tmp(:,3) = abs(xcorr(outarray(:,3),(ft))*ts)/mtmp;
tmp(:,4) = abs(xcorr(outarray(:,4),(ft))*ts)/mtmp;

P = 4;
figure(1);
for ii = 1:P
    subplot(P,1,ii);
    plot(ax,real(outarray(:,ii)));
end

ax1 = linspace(-length(tmp)/2,length(tmp)/2,length(tmp));
ax1 = ax1*ts*B;
figure(2);
for ii = 1:P
    subplot(P,1,ii);
    plot(ax1,tmp(:,ii));
end

figure(3);
plot(ax1,tmp(:,1),ax1,tmp(:,2),ax1,tmp(:,3),ax1,tmp(:,4))
xlabel('t (in seconds)');
ylabel('Relative Amplitude');
grid
axis([-5 5 0 1])

```

% A Matlab code to compare the loss in SNR between using time-varying phase weights and constant phase weights
 %for receive, and constant phase weights for both transmit and receive.

```
load fixedTxAndRx0To60deg50percentbandwidth.mat
```

```

% Extract the SNR Loss
tmp1 = zeros(size(tmp));
tmp2 = zeros(lenM,1);
mf = zeros(length(outarray)*2-1,lenM);
for ii = 1:lenM
    mf(:,ii) = abs(xcorr(outarray(:,ii),(ft))*ts)/mtmp;
    tmp1(:,ii) = 20*log10(mf(:,ii));
    tmp2(ii) = max(tmp1(:,ii));
end

```

```
tmp2a = tmp2;
```

```
load fixedTxAndRx0To60deg65percentbandwidth.mat
```

```

% Extract the SNR Loss
tmp1 = zeros(size(tmp));
tmp2 = zeros(lenM,1);
mf = zeros(length(outarray)*2-1,lenM);
for ii = 1:lenM
    mf(:,ii) = abs(xcorr(outarray(:,ii),(ft))*ts)/mtmp;
    tmp1(:,ii) = 20*log10(mf(:,ii));
    tmp2(ii) = max(tmp1(:,ii));
end

```

```
tmp2b = tmp2;
```

```
load fixedTxAndRx0To60deg80percentbandwidth.mat
```

```

% Extract the SNR Loss
tmp1 = zeros(size(tmp));

```

```

tmp2 = zeros(lenM,1);
mf = zeros(length(outarray)*2-1,lenM);
for ii = 1:lenM
    mf(:,ii) = abs(xcorr(outarray(:,ii),(ft))*ts)/mtmp;
    tmp1(:,ii) = 20*log10(mf(:,ii));
    tmp2(ii) = max(tmp1(:,ii));
end
tmp2c = tmp2;

load TVWTxAndfixedRx0To60degat50percentbandwidth.mat

% Extract the SNR Loss
tmp1 = zeros(size(tmp));
tmp2 = zeros(lenM,1);
mf = zeros(length(outarray)*2-1,lenM);
for ii = 1:lenM
    mf(:,ii) = abs(xcorr(outarray(:,ii),(ft))*ts)/mtmp;
    tmp1(:,ii) = 20*log10(mf(:,ii));
    tmp2(ii) = max(tmp1(:,ii));
end

tmp2d = tmp2;

load TVWTxAndfixedRx0To60degat65percentbandwidth.mat

% Extract the SNR Loss
tmp1 = zeros(size(tmp));
tmp2 = zeros(lenM,1);
mf = zeros(length(outarray)*2-1,lenM);
for ii = 1:lenM
    mf(:,ii) = abs(xcorr(outarray(:,ii),(ft))*ts)/mtmp;
    tmp1(:,ii) = 20*log10(mf(:,ii));
    tmp2(ii) = max(tmp1(:,ii));
end
tmp2e = tmp2;

load TVWTxAndfixedRx0To60degat80percentbandwidth.mat

% Extract the SNR Loss
tmp1 = zeros(size(tmp));
tmp2 = zeros(lenM,1);
mf = zeros(length(outarray)*2-1,lenM);
for ii = 1:lenM
    mf(:,ii) = abs(xcorr(outarray(:,ii),(ft))*ts)/mtmp;
    tmp1(:,ii) = 20*log10(mf(:,ii));
    tmp2(ii) = max(tmp1(:,ii));
end
tmp2f = tmp2;

figure(1);
plot(rad2deg(M),tmp2a,'s-',rad2deg(M),tmp2b,'*-',rad2deg(M),tmp2c,'d-');
hold on
plot(rad2deg(M),tmp2d,'s-',rad2deg(M),tmp2e,'*-',rad2deg(M),tmp2f,'d-');

ylabel('Loss in SNR (in dB)');
xlabel('Scan Angle (in degs)');
grid;
legend('50% bandwidth','65% bandwidth','80% bandwidth');

```

% A Matlab code to simulate I & Q channels amplitude and phase mismatch for LFM signals
 % generated using specification of AD9854 (use worst case condition)

```

PW = 1e-6;      % Sweep period
BW = 10e6;      % Bandwidth of LFM
fc = 20e6;      % Sweep frequency
L0 = 1.9e9;     % Local oscillator
gain_diff = 0.5; % in dB
phase_diff = 1; % in deg

mu = BW/PW;
fs = 4*(BW/2+fc);
ts = 1/fs;
t = (0:ts:PW-ts)-PW/2;
signal = exp(j*2*pi*fc*t + j*pi*mu*(t.^2)); % actual signal
real_phase = angle(signal) + deg2rad(phase_diff);
real_amp = real(signal).*(10^(gain_diff/10))/cos(angle(signal));
real_signal = real_amp*cos(real_phase); % imbalance in the I
signal1 = real(signal) + j*imag(signal); % actual signal
signal = real_signal + j*imag(signal); % signal containing the imbalance in I
ll = length(signal);
u = fft(signal, 2048)/ll;
u1 = fft(signal1, 2048)/ll;
v = fftshift(20*log10(abs(u)));
v1 = fftshift(20*log10(abs(u1)));
ll = length(v);
range = (-ll/2:ll/2-1)/ll*fs + L0 ;

figure(1);
plot(range/1e6,v);
grid
xlabel('Frequency (MHz)')
ylabel('Amplitude (in dB)')

figure(2)
plot(range/1e6,v1)
grid
xlabel('Frequency (MHz)')
ylabel('Amplitude (in dB)')

```

APPENDIX B: PHASE RESPONSE OF DEMODULATOR WITH AGC MODE TURNED ON

The phase response of AD8347EVAL demodulator board with AGC mode turned on is tabulated in Table 7. Figure 32 shows a MATLAB plot for the measured differential I and Q components versus transmitted phase with AGC mode turned on. Figure 33 shows a plot of received phase versus transmitted phase with AGC mode turned on. Figure 34 shows a plot of the phase error versus transmitted phase with AGC mode turned on.

Transmit Phase (in degrees)	IOPP (VDC) voltage	IOPN (VDC) voltage	QOPP (VDC) voltage	QOPN (VDC) voltage
0	1.05881	0.96794	1.12181	0.90384
10	1.04828	0.97856	1.1205	0.90509
20	1.03912	0.98789	1.11871	0.90687
30	1.03074	0.99641	1.11617	0.90943
40	1.02214	1.0052	1.11203	0.9135
50	1.01015	1.01745	1.1046	0.92101
60	0.93772	1.09093	1.03458	0.9903
70	0.9189	1.10992	0.99557	1.02873
80	0.9153	1.11343	0.98679	1.0373
90	0.91265	1.11609	0.9776	1.04635
100	0.91264	1.11605	0.97764	1.0463
110	0.91103	1.1176	0.9674	1.076
120	0.91091	1.11778	0.9496	1.07396
130	0.91276	1.11597	0.94142	1.08211
140	0.92042	1.10823	0.91564	1.1079
150	0.99885	1.02876	0.8174	1.20476
160	1.01664	1.01064	0.80594	1.21604
170	1.01667	1.01066	0.80589	1.21603
180	1.01668	1.01067	0.80597	1.21606
190	1.04293	0.98389	0.79348	1.22819
200	1.0512	0.97552	0.79154	1.23014
210	1.05863	0.96804	0.79058	1.23111
220	1.06599	0.96069	0.791	1.23076
230	1.084	0.9426	0.79305	1.22887
240	1.21672	0.80787	0.8774	1.14544
250	1.24072	0.7836	0.93561	1.08785
260	1.24332	0.78088	0.9441	1.07941
270	1.24522	0.77898	0.95258	1.07094
280	1.24583	0.77831	0.96224	1.06145
290	1.24569	0.77845	0.97057	1.05322
300	1.2443	0.7798	0.97826	1.04565
310	1.24191	0.78228	0.98587	1.03817
320	1.23789	0.78654	0.9952	1.02906
330	1.20942	0.81542	1.04789	0.9769
340	1.0843	0.94224	1.1204	0.90544
350	1.0668	0.95994	1.12165	0.90399

Table 7. Measurement results of AD8347EVAL Quadrature demodulator board with AGC mode turned on.

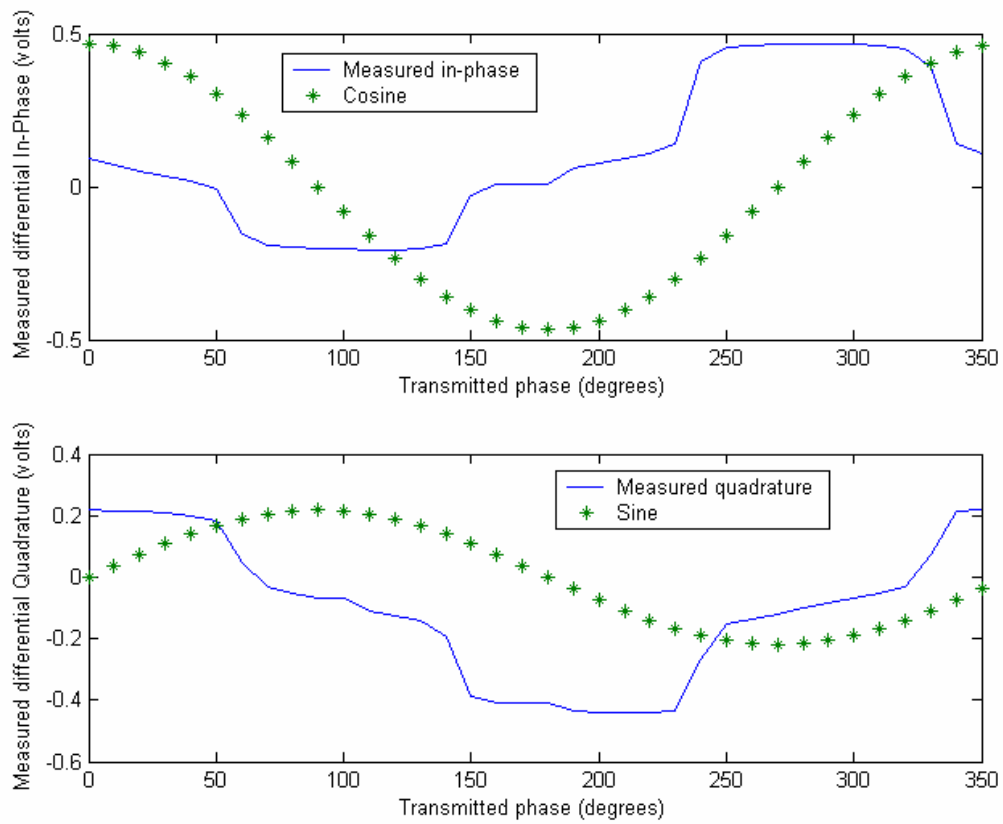


Figure 32. Measured Differential I and Q components versus transmitted phase with AGC mode turned on.

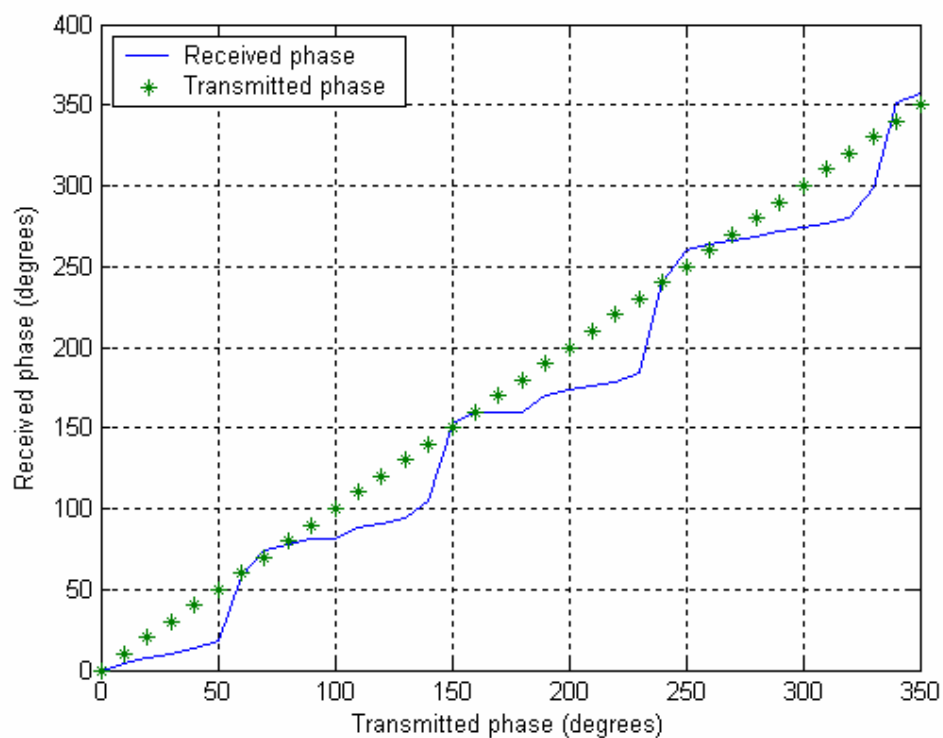


Figure 33. Demodulated phase versus transmitted phase with AGC mode turned on.

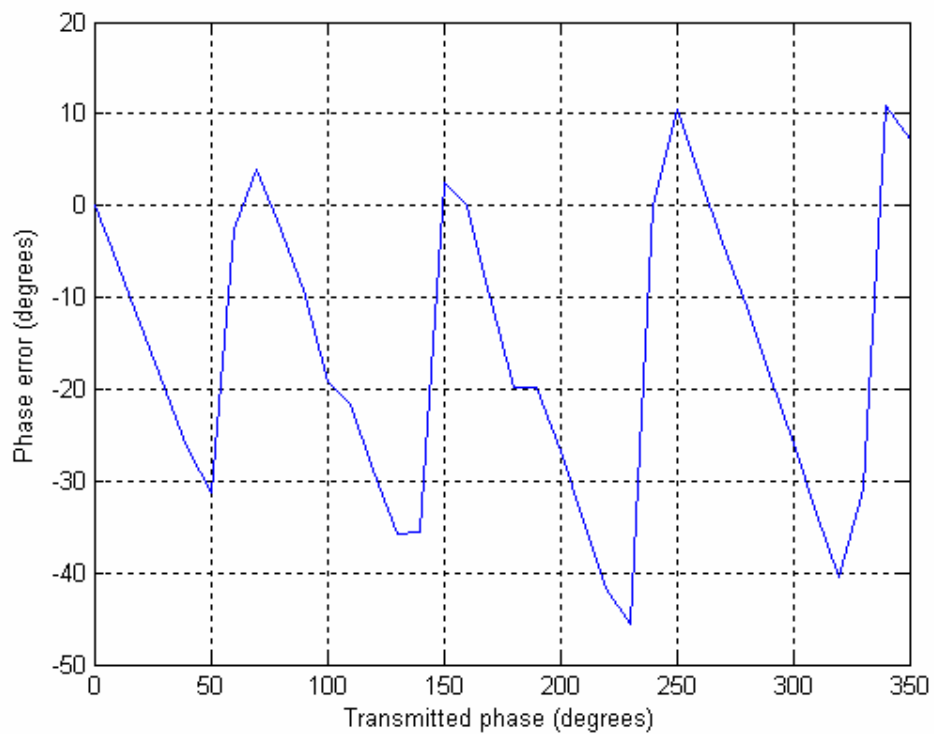


Figure 34. Phase error versus transmitted phase with AGC mode turned on.

LIST OF REFERENCES

- [1] U.S Navy Chief of Information, <http://www.chinfo.navy.mil/navpalib/policy/vision/vis02/vpp02-ch3e.html>, last accessed on September 2004.
- [2] M. I. Skolnik, *Introduction to Radar Systems*, 3rd edition, pp. 651- 661, McGraw Hill, New York, 2001.
- [3] L. C. Esswein, "Genetic algorithm design and testing of a random element 3-D 2.4 GHz phased array transmit antenna constructed of commercial RF microchips," Master's Thesis, Naval Postgraduate School, Monterey, California, June 2003.
- [4] Cher Sing Eng, "Digital antenna architectures using commercial off the shelf hardware," Master's Thesis, Naval Postgraduate School, Monterey, California, December 2003.
- [5] Richard G. Plumb, "Antenna Array Beam Steering Using Time-Varying Weights," *IEEE Transactions on Aerospace and Electronic Systems*, Vol. 27, No. 6, pp. 861-865, November 1991.
- [6] Richard G. Plumb, "Matched Filter Response of a Linear Array with Time-Varying Phase Weights," *IEEE Transactions on Aerospace and Electronic Systems*, Vol. 29, No. 3, pp. 1046-1050, July 1993.
- [7] John Litva and Titus Kwok-Yeung Lo, *Digital Beamforming in Wireless Communications*, pp. 16- 17, Artech House, Boston, 1996.
- [8] Robert J. Mailloux, *Phased Array Antenna Handbook*, pp. 29-37, Artech House, Boston, 1994.
- [9] Warren L. Stutzman and Gary A. Thiele, *Antenna Theory and Design*, 2nd edition, pp. 121- 122, Wiley, New York, 1998.
- [10] D. L. Miroslav, J. L. Milan, and O. L. Borislav, "Analysis of SDMA & smart antenna techniques for existing and new mobile communication systems," <http://www.telfor.org.yu/telfor2001/radovi/4-1.pdf>, November 2003, last accessed on September 2004.

- [11] Prof. Ethan Yuanxun Wang, Notes for EE262 (Antenna Theory & Design), UCLA, 2002 (unpublished), <http://www.ee.ucla.edu/~ywang/EE262/notes.htm>, last accessed on September 2004.
- [12] Dan P. Scolnik and J. O. Coleman, "Optimal design of wideband array patterns," *Proceedings of IEEE International Radar Conference*, pp. 172-177, 2000.
- [13] Analog Devices AD8347 Quadrature Demodulator, http://www.analog.com/UploadedFiles/Data_Sheets/756258393AD8347_0.pdf, November 2003, last accessed on September 2004.
- [14] Rick Cushing, "Single-Sideband Upconversion of Quadrature DDS Signals to the 800-to-2500 MHz," *Analog Dialogue*, Volume 34, Number 03, May, 2000.
- [15] Analog Devices AD9854 Direct Digital Synthesizer, http://www.analog.com/UploadedFiles/Data_Sheets/172781686AD9854.pdf, October 2004, last accessed on September 2004.
- [16] John Van Nierop, "Design of microstrip transmission lines using PCB laminates," a mathcad program, <http://www.circuitsage.com/tline/pcbtrans.mcd>, last accessed on October 2004.
- [17] Jeff Corbin and Robert L. Howard, "TDU Quantization Error Impact on Wideband Phased-Array Performance," *Proceedings of IEEE International Conference on Phased Array Systems and Technology 2000*, pp. 457- 460, Dana Point, California, May 2000.
- [18] Daniel J. Rabideau, "Improved Wideband Time Delay Beam-Steering," *Proceedings Thirty-fifth IEEE Asilomar Conference on Signals, Systems and Computers*, Vol. 2, pp. 1385-1390, Pacific Grove, California, November 2001

INITIAL DISTRIBUTION LIST

1. Defense Technical Information Center
Ft. Belvoir, Virginia
2. Dudley Knox Library
Naval Postgraduate School
Monterey, California
3. Chairman, Electrical & Computer Engineering Department
Code EC
Naval Postgraduate School
Monterey, California
4. Professor David C. Jenn
Code EC/Jn
Naval Postgraduate School
Monterey, California
5. Professor Jeffrey B. Knorr
Code EC/Ko
Naval Postgraduate School
Monterey, California
6. Professor Yeo Tat Soon
Director, Temasek Defence Systems Institute
National University of Singapore
Singapore
7. Professor Michael Melich
Wayne E. Meyer Institute of System Engineering
Naval Postgraduate School
Monterey, California